Published in final edited form as:
Reprod Toxicol. 2017 June ; 70: 82–96. doi:10.1016/j.reprotox.2017.05.005.

EMBRYONIC VASCULAR DISRUPTION ADVERSE OUTCOMES: LINKING HIGH THROUGHPUT SIGNALING SIGNATURES WITH FUNCTIONAL CONSEQUENCES

Robert G. Ellis-Hutchings[*,1], **Raja S. Settivari**[*], **Alene T. McCoy**[*], **Nicole Kleinstreuer**[†], **Jill Franzosa**[‡], **Thomas B. Knudsen**[‡], **Edward W. Carney**[*]

[*]Toxicology and Environmental Research and Consulting, The Dow Chemical Company, 1803 Building, Midland, MI 48674;

[†]National Toxicology Program Interagency Center for Evaluation of Alternative Toxicological Methods, Research Triangle Park, North Carolina, 27711;

[‡]National Center for Computational Toxicology, Office of Research and Development, United States Environmental Protection Agency, Research Triangle Park, North Carolina, 27711

Keywords

5HPP-33; TNP-470; Embryo; Vascular Disruption; ToxCast; Functional In Vitro Assay

Introduction

Embryonic vascular disruption is an important adverse outcome pathway (AOP) given the knowledge that chemical disruption of early cardiovascular system development leads to broad prenatal defects. The cardiovascular system is the first functional organ system to develop in mammals [1]. The primary vasculature differentiates from angioblasts to form the primitive vascular plexus in the early embryo and visceral yolk sac (vasculogenesis). These systems undergo subsequent remodeling and expansion (angiogenesis) to form the mature cardiovascular system [1]. Since numerous biological processes are linked to vascular development, *in utero* vascular disruptions are thought to be associated with a variety of birth defects and pregnancy complications [2] ranging in nature and severity from embryolethality [3] to preeclampsia [4], microphthalmia [5], and limb defects [6] to name a

[1]Corresponding author: Toxicology and Environmental Research and Consulting, The Dow Chemical Company, 1803 Building, Midland, MI 48674. Rellis-hutchings@dow.com.

5.0 Conflict of interest

There are no conflicts of interest to report. This work was sponsored through Strategic Research Project (SRP) funding at The Dow Chemical Company. Collaboration with the U.S. Environmental Protection Agency and the National Toxicology Program was made possible by joint agreement to the work product scope.

6.0 Dedication

This publication is dedicated to the late Dr. Edward Carney whose devotion to the fields of developmental and predictive toxicology has impacted a great many scientists during his life. He will always be remembered as an excellent scientist, mentor, and friend.

few. Vascular disruption was identified as one of 6 teratogenic mechanisms linked with medications taken by women of childbearing potential [7]. In humans, the most common apparent cause of limb deficiencies was found to be vascular disruption defects [8]. Susceptibility to thalidomide was linked to the disruption of immature angiogenic network at time of exposure [9]. Predicted vascular disrupting chemicals in ToxCast correlate with developmental toxicity [10]. Finally, many genetic and environmental factors can alter molecular pathways regulating angiogenesis [11].

Development of high-throughput screening (HTS) and *in vitro* profiling assays in recent years has generated advances towards providing the experimental throughput, target specificity, and computational capabilities necessary to thoroughly investigate vascular developmental toxicity. For example, the US EPA's ToxCast program and the Tox21 consortium generate *in vitro* HTS data on 1000's of chemicals against 100's of molecular targets and biological pathways [12] [13]. These HTS data facilitate chemical hazard identification to support chemical prioritization efforts for further evaluation under existing regulatory requirements (e.g. Endocrine Disruptor Screening Program), establishment of AOPs for toxicity mechanisms, and development of computational predictive models for these mechanisms. Predictive models for prenatal developmental toxicity [14] as well as disruptions in embryonic vascular development [11, 15] were recently developed, using this large *in vitro* dataset to build mechanistic understanding of adverse developmental outcomes.

One potential challenge with building predictive models from the existing HTS dataset is that the vascular disruption assays within the ToxCast and Tox21 programs (ToxCastDB, http://epa.gov/ncct/toxcast/data.html) consist mainly of cell-based or cell-free biochemical endpoints targeting specific molecular regulators of vasculogenesis or angiogenesis [10]. In contrast, most *in vivo* developmental toxicity assays, particularly regulatory guideline studies such as those compiled in US EPA's Toxicity Reference Database (ToxRefDB, http://actor.epa.gov/toxrefdb/faces/Home.jsp), are based on descriptive, apical endpoints which have little depth or detail for specific mechanisms of action. To evaluate the predictive capability of the ToxCast and Tox21 program assays, there is a need for an intermediate tier of functional assays that provide more specific information on vascular disruption and resulting adverse outcomes. In vitro functional assays of intermediate complexity, while lower in throughput, may bridge to in vivo predictivity through incorporation of multiple cell types, use three-dimensional cultures, include microfluidics apparatuses, and/or use ex vivo tissues. Examples where intermediate functional assays have shown utility include improved drug liability in safety assessments for cardiovascular [16] and drug-induced liver injury [17].

In the present study, we conducted an intermediate tier of assays to help bridge our understanding of vascular disruption effects, using vascular outgrowth and embryonic development assays as a proof of concept. The rat aortic explant assay (AEA) was included as a prototypical angiogenesis assay [18] while the rat whole embryo culture (WEC) assay and zebrafish developmental toxicity (ZET) assay were included to assess embryo development [19, 20]. The WEC assay has played a pivotal role in advancing our knowledge of normal embryonic development evidenced by the role it played in studies of normal

gastrulation [21], neural tube formation [22], craniofacial development [23, 24], and cardiac development [25], just to name a few. The WEC and ZET intact embryo assays have been shown to have test accuracies for in vivo teratogencity prediction of 68–80% and 75–92% [26], respectively, and been previously used to assess vascular remodeling, endothelial cell proliferation, placental development, and vessel disruption [27–31]. Results obtained in the AEA, WEC, and ZET assays can be related back to the HTS data to support further assessment of how well the ToxCast data may predict vascular disruption. Dose-response data derived from this study may assist interpretation of HTS assay results, particularly in benchmarking for positive responses. We tested the hypothesis that compounds predicted by ToxCast and Tox21 HTS assays to be putative vascular disrupting compounds (pVDCs) as a result of their high vascular bioactivity toxicological prioritization index (ToxPi) score [10, 11, 15], would demonstrate developmental toxicity and vascular disruption in the selected intermediate tier assays mentioned above. An additional goal of the research was to understand if the developmental toxicity was a consequence of vascular disruption or an alternative mechanism of action. Here, we evaluated two anti-angiogenic compounds with high ToxPi pVDC scores and differing mode(s) of action, 5HPP-33 and TNP-470, in the three functional assays mentioned above.

The two compounds selected as a proof of concept for embryonic vascular disruption include a synthetic thalidomide analogue (5HPP-33) and a synthetic fumagillin analogue (TNP-470). Although *in vivo* data in mammalian systems or humans are not available for 5HPP-33, thalidomide is well known both for its anti-angiogenic[32] and teratogenic [33] properties. Across a number of synthetic thalidomide analogues, 5HPP-33 showed the most potent anti-angiogenic activity in HUVEC cells [32]. Other thalidomide derivatives are well studied for their vascular developmental toxicity (e.g., CPS49), with primary findings being the prevention of blood vessel outgrowth and remodeling, loss of angiogenic vessels, and induction of limb reduction defects in chick embryos [9]. Proposed modes of action of 5HPP-33 include alteration of tubular polymerization [34–36], inhibition of mitosis [35], induction of apoptosis [37], extracellular matrix remodeling [15, 34], and inhibition of NF-κB [38]. TNP-470 was developed as an anti-angiogenic cancer therapeutic agent with a reduced preclinical toxicity profile to replace the antifungal, fumagillin [39]. Tumor growth and angiogenesis is inhibited by TNP-470 in mice bearing Lewis lung carcinoma cells [40] and while *in vivo* developmental data in mammalian systems is not available from regulatory guideline toxicity studies, TNP-470 administered to mice caused microphthalmia and reduced hyaloid vessel length in one study [5] and disrupted placental development resulting in complete embryonic resorptions in another [41]. In the latter study, decreased embryo blood vessel density was observed in an intermediate timepoint following TNP-470 administration. TNP-470's suspected mode of action includes disruptions of methionine aminopeptidase II (MetAP2) in vascular endothelial cells resulting in their cytostatic growth arrest [42]. Experiments with microtubule-associated protein 2 (MAP2) conditional knockout mice and MAP2-null lines further indicate a role for MetAP2 in early embryonic development as well as in a p53-dependent gastrulation checkpoint [43]. While it was hypothesized that both 5HPP-33 and TNP-470 would induce developmental toxicity and vascular disruption in the selected intermediate tier assays, the separate anti-angiogenic mechanisms of action for these pVDCs should result in distinct effects on embryonic

development. This paper is part of a larger research program focusing on validation/qualification of pVDC signatures in varying model systems including: evaluation of the ToxCast Phase I [44] and ToxCast Phase II chemical libraries using zebrafish, human endothelial cells [45], and an RNAseq analysis of 5HPP-33 and TNP-470 in culture rat embryos [46] with the parallel goal of an AOP Wiki developed for this pathway (https://aopwiki.org/wiki/index.php/Aop:43).

MATERIALS AND METHODS

Chemicals

5HPP-33 (H9415, Lot number 09K46131; CASRN 105624-86-0) and TNP-470 (T1455, Lot number 021M4609V; CASRN 129298-91-5) were obtained from Sigma-Aldrich Chemical Company (St. Louis, Missouri) and had purities of ≥ 98%.

Animal husbandry

All animal studies described in this paper were performed at The Dow Chemical Company (Midland, MI). The laboratory is fully accredited by the Association for Assessment and Accreditation of Laboratory Animal Care (AAALAC) International and all animal procedures were reviewed and approved by the Institutional Animal Care and Use Committee (IACUC) at The Dow Chemical Company. Nulliparous adult female Crl:CD(SD) rats (Charles River Breeding Laboratories, Portage, MI) were used in AEA and WEC experiments while New Zealand White rabbits (Covance Research Products, Kalamazoo, MI) were used in AEA experiments. Rats used in the WEC experiments were time-mated at the breeders' facilities. In order to promote uniformity in stage of embryo development, mating was restricted to approximately three hours (4–7 p.m.) and the following day was considered gestation day (GD) 0. The animals were housed singly in stainless steel cages in rooms designed to maintain environmental conditions for temperature (22±3 °C for rats, 20±1 °C for rabbits), humidity (40–70% for rats, 40–60% for rabbits), and photocycle (12-hour light/dark). Rats were housed either in wire bottom cages suspended above catch pans or in solid bottom cages with absorbent bedding. Cages contained a hanging feeder and pressure-activated lixit valve-type watering system. Environmental enrichment for the rats included non-woven gauze placed in the cages (wire bottom cages) or use of ground corn cob and shredded Aspen bedding and open areas on the cage sides for visualization of other rats (solid bottom cages). Rabbit cages had flattened tube grid floors suspended above catch pans with absorbent non-contact bedding, with a J-type feeder and a pressure activated lixit valve-type watering system. There was a variety of stainless steel objects attached to the front of the cages for environmental enrichment. Rats were maintained on LabDiet Certified Rodent Diet #5002 (PMI Nutrition International, St. Louis, MO) while rabbits were maintained on Purina Certified Laboratory Rabbit Chow No. 5325 (Ralston Purina Co, St. Louis, MO). All animals were provided municipal water. A cage-side examination of all animals was conducted twice daily.

ToxCastDB

All *in vitro* data for the current work was extracted from chemical-bioactivity effects data in ToxCastDB (release date October 2015). Detailed descriptions of the ToxCast and Tox21

assay sets and their data management approaches are available elsewhere (http://actor.epa.gov/actor/faces/ToxCastDB/Home.jsp, http://www.epa.gov/ncct/toxcast/,[47], http://epa.gov/ncct/Tox21/). This large dataset contains *in vitro* biological screening data on 1,860 chemicals tested through a battery of molecular and cellular HTS experiments [12] and provides an opportunity to develop predictive signatures of diverse chemical-bioactivity relationships in prenatal developmental toxicity [14]. The ToxCastDB version for the present study included 888 HTS assay endpoints from 11 high throughput assay technology platforms pointing to a range of high-level cell responses and approximately 300 signaling pathways (BioAssay Ontology version 2.0). Some molecular targets among the 293 annotated in ToxCastDB were assayed in several different platforms (orthogonal) whereas others may have been unique to a technology platform. The data processing pipeline (http://epa.gov/ncct/toxcast/data.html) included raw data Q/A checks, normalization, automated curve fitting, visual plots of the concentration-response relationships, and calculation of concentration causing half maximal response in activity (AC50) or the Lowest Effect Concentration (LEC). Table 1 includes brief descriptions of the ToxCast Phase II and Tox21 assay data and test concentrations evaluated in this study. All assay data is publicly available as both a series of flat files (http://epa.gov/ncct/toxcast/data.html) and online at (http://actor.epa.gov/dashboard/). Assay responses were considered “active” if either the Hill or gain-loss model could be fit and the observed response met an efficacy cutoff. Further expert review of the individual chemical-assay outputs were performed for assay responses flagged as potential false positives/negatives (http://epa.gov/ncct/toxcast/files/MySQL%20Database/Pipeline_Overview.pdf). In a few instances this led to the reversal of “active” calls. Analysis of cytotoxicity-associated activity in the ToxCast assays was performed similarly to Judson and colleagues [48]. Statistical comparison of the mean AC50 values between 5HPP-33 and TNP-470 was conducted using unpaired t-tests.

An initial analysis of the ToxCast data revealed a number of critical vascular signaling targets *in vitro* that were disrupted by chemicals with known developmental toxicity *in vivo* [10]. These bioactivity patterns helped identify multiple targets in inflammatory chemokine signaling, extracellular matrix remodeling, and vascular growth factor regulation that were further expanded and cross-referenced with vascular phenotypes from genetic mouse models [11]. The resulting group of HTS assays targeting critical vascular signaling molecules can be used to rank chemicals based on a toxicological prioritization index, or ToxPi, whose slices correspond to the magnitude of the chemical perturbation for that particular target. The calculated pVDC score is relative to the entire area of the circle (i.e. pVDC = 1 would require full potency in every assay in ToxPi), and the highest scoring chemical in the Phase I and II library had a score of 0.498 [45, 49]. These assays are all mapped as potential molecular initiating events or cellular key events in the proposed AOP for embryonic vascular disruption leading to developmental toxicity [11].

Whole embryo culture

Intact rat conceptuses were isolated and cultured similar to the methods of [50] and [51]. On GD 10.0, untreated, pregnant rats were placed into an inhalation chamber containing a continuous flow of carbon dioxide/oxygen (CO_2/O_2) to induce deep narcosis and were euthanized *via* cervical dislocation. Briefly, conceptuses were dissected free of decidual

tissue and Reichert's membrane, leaving the visceral yolk sac and ectoplacental cone intact using aseptic technique. Early-somite stage embryos that appeared viable and at a uniform stage in development were transferred to culture bottles (2 embryos/bottle) containing pre-warmed, pre-gassed control culture media. The culture medium was comprised of 50% (v/v) heat-inactivated (30 min, 56 °C), filter-sterilized rat serum and 50% Waymouth's medium (Invitrogen, Grand Island, New York) with antibiotics (penicillin 5 IU/mL and streptomycin 10 μg/mL; Invitrogen, Grand Island, New York). On the morning of culture initiation, the culture media pH was adjusted to 7.2–7.4 ± 0.1 using either 0.1 M HCl or 50% NaOH, aliquoted into sterile culture bottles, and equilibrated to the specified incubation conditions (see below) for at least 20 min prior to adding embryos. Upon addition to the culture media, embryos were equilibrated for at least 1 h before treatment.

The culture bottles were maintained in a continuous flow rotating culture unit (BTC Engineering, Cambridge, UK) for up to 48 h at 37 °C with a humidified gas atmosphere composed of 5% CO_2, 20–95% oxygen (increased as development advances) and 75–0% nitrogen (gas mixture flow rate ≈ 20 ml/min.). Embryos from each litter were distributed in relatively equal proportions between control and treated groups to control for any litter-effect bias. Treatment was achieved by diluting a 10× stock solution prepared in culture medium into the culture bottle to achieve a final concentration of 1.6 – 46.0 μM (5HPP-33) or 0.001–10.0 μM (TNP - 470) in a total volume of 2 mL/bottle (n=16/group unless otherwise indicated) (Table 1). Test concentrations were determined based upon the results of preliminary dose range-finding experiments aimed at identifying concentrations inducing some toxicity but not an excessive amount.

Following the culture period, the intact conceptuses were evaluated for viability (presence of a heart beat) and morphology based upon the method of [52]. Briefly, standard developmental morphology scores were assigned for a variety of embryonic structures, which were added together to make up the total morphology score for each embryo, respectively. The evaluated embryonic structures included: visceral yolk sac (VYS) circulation, VYS vessels, allantois, heart, flexion, caudal neural tube, forebrain, midbrain, hindbrain, otic system, optic system, olfactory system, branchial bars, maxillary process, mandibular process, forelimb, hindlimb, and somites.

The embryos and VYS were then dissected apart, washed through several changes of ice cold PBS and transferred separately to microcentrifuge tubes containing 500 μL of distilled deionized water. The samples were then used to determine the protein content [53] using bovine serum albumin (BSA; Sigma Chemical Company, St. Louis, Missouri) as the standard for normalization. RNA from the embryos and VYS were collected for RNAseq analysis in a companion paper [46].

Rat and Rabbit Aortic Explant Assay

Descending aorta from adult rats and rabbits were excised and cut into equally sized explants and cultured in a three dimensional matrix *in vitro* in 6- or 24-well plates, followed by microvessel outgrowth (reflective of angiogenesis) quantification at the end of the culture. Measurement of cell viability was also conducted to assess whether any effects

observed in the assay were due to cytotoxicity, rather than alterations in vascular outgrowth. Details on the assay procedures are provided below.

In a sterile container on ice, cold rat tail collagen I (5 mg/ml, Gibco, Invitrogen Corp.) was prepared according to the protocol from Invitrogen. For a total volume of 25 ml, 15 ml collagen was added to 7.125 ml sterile distilled H2O, 0.375 ml NaOH and 2.5 ml 10× PBS. The final concentration of collagen I was 3.2 mg/ml. The collagen was pipetted into the wells of a 24-well plate and incubated at approximately 37°C, 95% humidity for 30–40 min until a firm gel was formed. The wells were rinsed once with PBS before adding aortic explants.

Aseptic aortic tissue was washed in cold sterile PBS or endothelial basal medium. The peri-aortic fibroadipose tissue was removed with fine microdissecting forceps. Aortae were sectioned into ~1.5 mm segments using biopsy punches. The explants were rinsed five times consecutively with sterile PBS then placed in the previously-prepared wells containing 3D collagen gel (one per well). The explants were covered with an additional volume of liquid (cold) collagen I solution then incubated at 37 °C, 5% CO2/95% humidity for 30–40 minutes until the top portion of the gel became solid (test day (TD) 1). Control medium was added to the wells, and the explants were incubated at 37 °C until the initiation of visible microvessel outgrowth from the aorta biopsy (three days in the current experiments). On TD 4, the media was removed and new media was added containing the appropriate treatment (Table 1), and the explants were incubated for 4 additional days (until TD 8). This duration allowed for maximal microvessel outgrowth while still being able to capture and analyze the entire image area.

Beginning on TD 4, the explants were imaged every day using an Olympus DP70 high-resolution (12.5 megapixel) digital camera mounted on a Leitz Diavert inverted microscope with Olympus DP-BSW image acquisition software (v2.01). Total magnification was 14× (Brightfield 1.4× objective lens, Periplan 10× eyepiece), and the microscope was fitted with a Leitz Illumination Transformer (Model 050250). The aortic explant images on TD 8 were captured under the same observation conditions and used to perform image analysis. Microvessel outgrowth was quantified by image analysis of the photomicrographs using Image J software. (version 1.44p, National Institutes of Health, USA). Initial analysis included background subtraction and generation of binary images for each explant followed by calculation of the raw integrated densities by summing values of the pixels in the image or selection area. To determine the signal specifically from the vessel sprouting, integrated density of the TD 4 explant was subtracted from the integrated density value of the same explant captured on TD 8. This normalization step enabled subtraction of the signal derived from the respective explant itself as well as the signal resulting from collagen matrix. The quantified assessment of microvessel outgrowth per explant was calculated as the mean and standard deviation of the integrated density score of the explants (n = 3–12) per treatment group. Differences in microvessel integrated density between dose groups was determined by statistical analysis of variance approach using Graphpad (Version 5.04).

A cytotoxicity assay (CytoTox-Fluor Assay, Promega, Madison, Wisconsin) was conducted to evaluate the potential contribution of cytotoxic effect on changes in vascular outgrowth.

The assay uses a fluorogenic peptide substrate (bis-alanyl-alanyl-phenylanlanyl-rhodamine 110 (bis-AAF-R110)) to assess activity of a distinct cytotoxicity-associated protease that is released from cells that have lost membrane integrity. The fluorescence produced is proportional to the number of dead cells. The cytotoxicity assessment was conducted after 24 (TD 5) and 48 hours (TD 6) of incubation with the treatments, according to the manufacturer's protocol. In brief, 100 μL of media from each aortic explant well (n=3–5/ treatment group) was transferred to three wells of a 96-well plate, followed by addition of 100 μL of substrate and incubated for 1 h at 37 °C. Fluorescence was quantified using a FLUOstar OPTIMA fluorescence plate reader (BMG Lab technologies) at 485 nm as the excitation and 520 nm as the emission wavelength. The values were background-subtracted and normalized to controls. Differences in fluorescence between dose groups were determined by statistical analysis of variance approach using Graphpad (Version 5.04).

Zebrafish Embryotoxicity Assay

Adult tropical wild-type outbred pondfish zebrafish (*Danio rerio*) (Aquatic Research Organisms, Hampton, NH) were maintained and spawned in accordance with IACUC approval and standard operating procedures at The Dow Chemical Company. Adults were maintained on a 14/10 h light-dark schedule on a recirculating system in which water was maintained at 28 ± 2°C and pH 7.0–7.5. Viable zebrafish embryos collected from spawning adult fish were exposed to 5HPP-33 or TNP-470 in 0.5× E2 culture buffer [54] from approximately 1 to 4 h post fertilization (hpf) until −120 hpf (day 5) at up to seven test concentrations/chemical (Table 1) plus a vehicle control (n = 10 – 12 embryos/ concentration/replicate). Testing was conducted under static exposure conditions in 24-well plates containing 1 mL of the appropriate dosing solution and covered with self-adhesive transparent plate seal (Nunc, Roskilde, Denmark). There were at least two independent assay replicates conducted per compound. During the five day culture, the embryos progress from the late cleavage stage through complete organogenesis [55, 56]. Using a streamlined approach from published methods [57], all embryos were evaluated for viability and for the presence or absence of abnormal development at characterized morphological locations at ~120 hpf. Morphological parameters evaluated included the brain, upper face (eye and sacculi/otoliths), lower face (upper and lower jaw and pharyngeal arches), heart, fins, somites, body axis/tail, and notochord [20],[58, 59]. An embryo was considered abnormal if one or more of the eight morphological locations was identified as such. The percentage of non-viable and abnormal embryos at ~120 hpf for each technical replicate were then calculated for the control and treated groups, and nonlinear regression analysis was used to estimate the concentration lethal to 50% of the embryos (LC_{50}) and that caused at 50% incidence of abnormal embryos (EC_{50}) using nonlinear curve fitting software [60].

RESULTS

5HPP-33

ToxCast HTS Assays/Vascular Disruption Signature—5HPP-33 was included in 887 ToxCast Phase-II assays with provisional AC50s in 202 (22.8%) of the assays (Table 2). The range of activity across the 202 assays in which 5HPP-33 was positive was 0.168 to 139 μM (Supplemental Table 1) with a median AC50 value of 18.7 ± 30.0 μM. 5HPP-33 was

active in all assay types (cell-free biochemical assays, cell-cell interactions in a co-culture system, transactivation assays, protein-fragment complementation, cytotoxicity, etc.) with the exception of the NCCT assay platform. The first 25th percentile of AC50 values, a reflection of the most sensitive assay responses to 5HPP-33, included 47 assay endpoints with an AC50 range of 0.168 to 7.566 μM (Table 3A) and a median AC50 value of 3.63 ± 2.2 μM. Notable among the most sensitive assay endpoint targets to 5HPP-33 were 12 related to the estrogen receptor steroid hormone activity, cell growth regulation (PI3K enzymatic inhibition, nuclear p53 accumulation, decreased proliferation, mitochondrial and cell cycle arrest), endothelial cell-related signaling (ER1 transactivation, decreased P-selectin), and inflammatory cytokine signals (MCP1, IL8). The AC50 values for all 202 assays where 5HPP-33 showed activity, with the assay descriptor, can be found in Supplemental Table 1.

None of the assays in the current ToxCast portfolio included direct vasculogenesis or angiogenesis assays. As such, the response profile of 5HPP-33 on these complex processes was predicted by a ToxCast signature based on the potential vascular disruption (pVDC) score [11, 49, 61]. The pVDC score for 5HPP-33 was 0.257, ranking 118 of 900 chemicals for which a pVDC score could be generated (1076 chemicals total, where 176 were inactive against all assays in the signature) [45]. While 5HPP-33 showed broad activity across assay endpoint targets, an assay platform which showed particular activity enrichment was the BioSeek platform, a cellular HTS model relevant to vascular disruption (Supplemental Table 1). This human primary cell co-culture platform uses human endothelial and other cell types to assess for functional responses such as pro-inflammatory/anti-angiogenic chemokine signaling, vascular endothelial growth factor (VEGF) signaling, and the plasminogen activating system (PAS) of enzymes and growth factors mediating matrix remodeling [62, 63]. 5HPP-33 showed broad activity in 65 of the 174 (37.4%) Bioseek assays at a median AC50 value of 15.2 ± 9.2 μM (Figure 1A). The compound was anti-proliferative to endothelial cells and showed a signal of effect on the targeted biomarker measures for cell-cell signaling at concentrations below those showing effects by the sulforhodamine B (SRB) cytotoxicity assay [64]. In that assay, 5HPP-33 induced cytotoxicity between 10.3 and 38.4 μM (mean = 11.9 μM), most notably in vascular cells and fibroblasts, but less so in T-cells and smooth muscle cells (Supplementary Fig 1A). The median of the log(AC50) for cytotoxicity assays across ToxCast following 5HPP-33 treatment was 18.6 μM (Supplementary Fig 1B) [48].

Rat Aortic Explant Assay—5HPP-33 dramatically disrupted microvessel outgrowth in rat aortic explants at concentrations > 0.46 μM, with complete attenuation at > 46 μM and an EC_{50} value of 1.28 μM (Figure 2A) (Table 4). The cellular morphology in the explants appeared disorganized and/or degenerate (Figure 3C and 3D). Cytotoxicity was not observed in the aortic explants at 4.6 μM but was at concentrations ≥ 46 μM (Supplementary Fig 1C), consistent with the BioSeek SRB and overall ToxCast assay findings.

Rat Whole Embryo Culture—The critical effect associated with *in vitro* exposure of early rat embryos to 5HPP-33 was reduced embryo viability by 48 h of culture (Figure 4A). The no-observable-effect-concentration (NOEC) for viability was 5.0 μM; embryolethality

was dose-dependent with no viable embryos at 46 μM and an LC50 = 21.2 μM. Due to the primary effect on embryo survival and demise of the cultured embryos exposed to 5HPP-33, we did not pursue a detailed characterization of the patterns of 5HPP-33 induced dysmorphology although earlier timepoints and intermediate doses. While not in viable embryos, yolk sac circulation/vascularity and allantois scores, and yolk sac diameter was unaffected by treatment (data not shown).

Zebrafish Embryotoxicity Assay—The critical effect associated with *in vitro* exposure of zebrafish embryos to 5HPP-33 was mortality by 120 hpf (Figure 4B). Although viability was statistically reduced at all treatment concentrations, the biologically-relevant NOEC for reduced viability was 0.1 μM. Above 0.1 μM, exposure to 5HPP-33 caused steep dose-dependent embryolethality as demonstrated by an LC50 = 3.41 μM and no viable embryos at 10 μM. Due to the primary effect on embryo survival and demise of the zebrafish embryos exposed to 5HPP-33, we did not pursue a detailed characterization of the patterns of 5HPP-33 induced dysmorphology. Notably, 5HPP-33 did not induce structural defects in the ToxCast zebrafish assays (Tanguay ZF, NHEERL ZF) and instead only caused lethality.

TNP-470

ToxCast HTS Assays/Vascular Disruption Signature—TNP-470 was tested in 876 ToxCast assays with AC50s in 82 (9.4%) of the assays (Table 2). The range of activity across the 82 assays in which TNP-470 was positive was 0.001 to 49.116 μM (Supplemental Table 2) with a median AC50 value of 6.6 ± 9.6 μM. TNP-470 was active in the Attagene (transcriptional activation), BioSeek (protein signaling in primary cells), NCCT (ATP viability assay), NovaScreen (cell-free biochemical), Odyssey Thera (cell signaling pathways), Tanguay ZF (zebrafish development), and Tox21 (ultra HTS) assay sets. The first 25^{th} percentile included 21 assays, with the majority from the BioSeek and Tanguay zebrafish platform, with an AC50 activity range of 0.001 to 3.434 μM (Table 3B) and a median AC50 value of 0.45 ± 1.3 μM, significantly lower than that of 5HPP-33 (Figure 1B). Notable among the first 25^{th} percentile AC50 values were 8 assay endpoints related to zebrafish development, nuclear receptor assay endpoints (PXR, FXR, AR), and within cell types related to vasculogenesis assay endpoints related to cellular regulation (cell proliferation), endothelial cell-related signaling (decreased P-selectin), tissue matrix remodeling (Collagen III), and inflammatory cytokine signals (NFkB, M-CSF, IL8) (Table 3B). The AC50 values for all 82 assays where TNP-470 showed activity, with the assay descriptor, can be found in Supplemental Table 2.

The vascular bioactivity score and ToxPi response profile for TNP-470 was recently evaluated to further assess its signature and potential to cause disruption of blood vessel formation and remodeling. The pVDC score 0.194 ranked this compound 190 of 900 ToxCast chemicals for which a score could be generated [49]. In the BioSeek assays, AC50 values were calculable for TNP-470 in 43 of the 174 assay endpoints (24.7%) (Table 2) and the median AC50 value was 6.19 ± 1.8 μM, statistically lower than 5HPP-33 (15.2 ± 9.2 μM) (Figure 1A). TNP-470 was anti-proliferative to endothelial cells, T cells and fibroblasts and showed anti-inflammatory, immunomodulatory, and tissue remodeling activities. TNP-470 activity in the BioSeek SRB cytotoxicity assay was limited to a single assay

endpoint, hDFCGF_SRB_down (decreased SRB in cytokine stimulated human neonatal foreskin fibroblasts) where the AC50 = 7.26 μM. The median of the log(AC50) for cytotoxicity assays across ToxCast following TNP-470 treatment was 4.27 μM (Supplementary Fig 2D).

Rat Aortic Explant Assay—TNP-470 treatment resulted in a 35–68% reduction in microvessel outgrowth across the tested concentrations, relative to controls, with an EC_{50} value of 0.018 μM (Figure 2B). Microvessel outgrowth was generally further reduced with increasing dose except at 0.0025 μM where a more moderate response was observed, likely due to variability across experimental replicates. The cellular morphology of the endothelial and stromal cells in the TNP-470 treated explants appeared normal compared to controls; however they had stunted microvessel growth (Figure 3E, F). This morphology differed from the more disorganized and/or degenerate phenotype noted in 5HPP-33-treated explants (compare Fig 3C, D with 3E, F). TNP-470 did not invoke cytotoxicity in aortic explants up to the highest tested concentration of 0.25 μM (Supplemental Figure 1E). These results show that TNP-470 stunts microvessel outgrowth in rat aortic explants at nM concentrations, which are 10- to 100× below cytotoxicity concentrations in this assay.

Rat Whole Embryo Culture—Exposure of early rat embryos to TNP-470 in WEC was dysmorphogenic. The percentage of abnormal embryos was increased at ≥ 0.025 μM TNP-470 up to 69% of embryos affected at 2.5 μM, with an EC50 = 0.038 μM (Figure 5A). Dysmorphogenesis was primarily characterized by defects in caudal extension and abnormal somite patterning, but also anterior defects were observed (Figure 6). Caudal extension defects primarily manifested as abnormally-shaped somites posterior to the forelimb bud with increasing severity caudally. Reductions in size and definition of the typical cuboidal shape were a prominent feature. Shortening of the overall length was common with reductions in the hindlimb primordia bud being apparent. Blistering was present on the tail and/or frontonasal process in about 25% of embryos. These results in cultured rat embryos show that exposure to TNP-470 induces clear dysmorphogenesis predominantly, but not limited to, the caudal region at non-embryolethal concentrations.

Zebrafish Embryotoxicity Assay—Developmental exposure of zebrafish to TNP-470 resulted in morphological defects at 120 hpf. As in the rat WEC experiments, this corresponded to an increase in the percentage of abnormal embryos at ≥ 0.01 μM TNP-470 with nearly 100% of the embryos affected at 10 μM and an EC50 = 0.032 μM (Figure 5B). Similar to rat embryos, zebrafish dysmorphogenesis was primarily characterized by defects in somite patterning and caudal extension (Figure 7). Abnormalities in caudal fin shape and disorganization of the characteristic chevron pattern were critical effects. Cardiac edema and retained yolk was a common finding at concentrations ≥ 0.1μM. Blistering in the forebrain, GI tract, and ventral surface was observed in about 5% of embryos at these concentrations. These zebrafish embryo results show that exposure to TNP-470 induces clear dysmorphogenesis at concentrations below which a more general effect on growth can be observed, and predominantly in the caudal region at non-lethal concentrations – similar to cultured rat embryos exposed to the compound. Furthermore, these findings were similar to TNP-470's activity in the Tanguay ZF ToxCast assay examining zebrafish development

regarding the affected assay endpoints and the concentration-response. Surprisingly, TNP-470 was inactive in the NHEERL ZF assay despite being tested up to 40 μM. The reason for this lack of activity is currently unclear.

DISCUSSION

In this study, we sought to test the hypothesis that compounds predicted by ToxCast and Tox21 HTS assays to be putative pVDCs (as a result of their high vascular bioactivity ToxPi score) would demonstrate developmental toxicity and vascular disruption in selected intermediate tier assays. Two known anti-angiogenic compounds with differing mode(s) of action, 5HPP-33 and TNP-470, were used in this proof of concept study to evaluate three functional non-HTS *in vitro* assays. Response profiles of the two compounds in the Phase II ToxCast HTS assays predicted the compounds to be pVDCs, consistent with their known potential for disruption of vessel formation [32, 40], but with distinct bioactivity patterns. Potency of theses pVDCs in the ToxCast HTS assays showed both substances to have median AC50 values in the low micromolar range with TNP-470 being approximately 3 times more potent than 5HPP-33 in its activity. In the functional follow-up assays, responses to 5HPP-33 treatment were similarly in the low micromolar range while TNP-470 was approximately 300 times more potent with responses in the nanomolar range (Table 4). Despite the difference in AC50 and EC50 values for TNP-470 between the functional, non-HTS assays and the ToxCast HTS assay set, the potency differences of the two compounds in the ToxCast BioSeek assay and the broader ToxCast 25th percentile AC50 responses were still statistically distinguished.

The potency similarity for 5HPP-33, but not TNP-470, between the ToxCast HTS assays and the functional follow up assays could lead one to suggest that for TNP-470 the ToxCast HTS assay set may not fully characterize this substance’s toxicity mode of action. Importantly however a few ToxCast assay/assay endpoints were capable of more specifically mirroring TNP-470’s nanomolar potency in the non-ToxCast functional assays, including two proliferation assay endpoints and 6 assay endpoints in the Tanguay Zebrafish assay.

Separate from potency differences between the two substances we sought to determine if these pVDCs demonstrated functional consequences, specifically, vascular disruption and developmental toxicity. Results from the rat AEA demonstrated the ability of 5HPP-33 and TNP-470 to disrupt vascular development. This explant assay simulates the *in vivo* angiogenesis environment by virtue of an intact tissue that includes the surrounding non-endothelial cells (such as smooth muscle cells and pericytes) and a supporting matrix [18]. Consistent with the ToxCast bioactivity profiles, distinct phenotypic responses were observed between the compounds in the rat AEA (Figure 3). Notably, TNP-470 was approximately 18–25-fold more potent in the AEA culture than the activity observed in the lower 25th percentile AC50 values for the BioSeek or ToxCast assays, respectively, with the exception of the above mentioned proliferation and Tanguay ZF assay endpoints. In contrast, 5HPP-33 disrupted microvessel outgrowth at concentrations similar to its observed activity in ToxCast HTS assays (Table 4). This may reflect a lack of assay coverage within the Phase II ToxCast assay set for the primary mode of action of TNP-470, methionine aminopeptidase II (MetAP2) inhibition [42] but reasonable coverage for the more diverse modes of action

for 5HPP-33 such as: tubular polymerization alterations [34–36], inhibition of mitosis [35], induction of apoptosis [37], extracellular matrix remodeling [15, 34], and inhibition of NF-κB [38].

An additional functional analysis used in this study was from embryo-based assays. Reconstructing the complexities of embryonic development through *in vitro* HTS assays is a challenge. The addition of two intact organism assays in this research, rat WEC and ZET assay, helps to address this challenge in integrated embryological systems. These incorporations are important since while HTS assays can be used to increase our understanding of the mechanisms of action associated with abnormal development and the role pVDCs play in this process, their predictive capability remain to be characterized in relation to *in vivo* embryonic development. Zebrafish screening is also a powerful tool for evaluating vascular morphogenesis during development (Tal et al. 2014). While *in vivo* data from regulatory guideline studies was lacking for these compounds, some *in vivo* data existed on these or similar chemicals to suggest their potential for adverse effects during development [9, 43, 65, 66]. In the current research, both compounds had adverse effects on embryonic development in the rat WEC and zebrafish ZET assays, with 5HPP-33 primarily causing embryolethality and TNP-470 causing dysmorphogenesis in the two species tested. Consistent with results from the rat AEA, the responses of 5HPP-33 were in the micromolar range, while TNP-470 was in the nanomolar range.

Cross-assay comparison for the zebrafish embryo assays revealed consistencies and differences between the assays. For 5HPP-33, the ZET and the two ToxCast assay endpoint sets (Tanguay_ZF, NHEERL ZF 144hpf) were consistent in their demonstration of lethality in the absence of malformations. The assay responses differed for 5HPP-33 regarding potency as both the ZET and the NHEERL ZF assays were similar while the Tanguay ZF assay was 6–8 times less potent. Interestingly, the Tanguay ZF assay volume is 0.1ml compared to 1ml or 0.25ml in the ZET and NHEERL ZF assays, respectively, indicating a possible contribution of treatment volume to these differences [67, 68]. Another variable between the assays, with less clear influence, is that both the ZET and NHEERL ZF assays use intact (non-dechorionated) embryos while the Tanguay ZF assay utilizes dechorionated embryos. For TNP-470, correlation between the ZET and the Tanguay ZF assay endpoints was strong both in terms of potency and developmental outcome. In both of these assays the zebrafish embryos responded in the low nanomolar range with structural abnormalities occurring in the absence of lethality. Surprisingly, TNP-470 was inactive in the NHEERL ZF assay despite testing up to 40μM. The reason for this lack of activity in the NHEERL ZF assay is not entirely clear, however it is the only zebrafish assay of the three with daily refreshing of the test media (instead of static exposure in the ZET and Tanguay ZF assays).

The embryolethality of 5HPP-33 observed here in whole embryo culture may be regulated through a systemic alteration in microtubule stabilization [36]. Colchicine, a known disruptor of microtubule stabilization, causes a high incidence of embryolethality [69, 70]. The ToxCast data for 5HPP-33 provide support for this with effects on cell growth regulation (PI3K enzymatic inhibition, nuclear p53 accumulation, decreased proliferation, mitochondrial and cell cycle arrest). It is also possible that a role for estrogen receptor signaling activity exists in the embryolethal effect as 14 estrogen receptor signaling targets

were among the most sensitive assay endpoint targets following 5HPP-33 treatment. It has been previously shown that embryos deficient in estrogen-related receptor beta (Esrrb) die before E10.5 due to severely impaired placental formation [71] and that Esrrb is an immediate target of Fgf/Mek signaling in trophoblast stem (TS) cells and in turn directly activates key TS cell genes [72].

The teratogenic effects observed with TNP-470 in the absence of embryolethality in the rat WEC and ZET assays have not been previously reported. These effects resemble somite and caudal extension defects seen with effectors of the Wnt signaling pathway [73, 74]. Knockdown of metap2 in zebrafish has been demonstrated to cause a tail extension defect in Wnt5 morphants [75], thereby providing indirect support for a Wnt-based mechanism of action of TNP-470. Using the selected intermediate functional assays, we confirm that 5HPP-33 and TNP-470, both predicted to be pVDCs in the ToxCast HTS assays, exhibit functional consequences of vascular disruption and developmental toxicity in *in vitro* assays.

Remaining questions to be addressed include whether vascular disruption with these prototypical VDCs is primary or secondary to the observed developmental toxicity and whether or not developmental toxicity occurs *in vivo*. Our results provide some insight to this question as both compounds produced developmental effects with a similar potency to that of vascular disruption in the AEA assay. For 5HPP-33, the ToxCast HTS assay data showed reasonable coverage for this substance with a strong ToxPi signature against the vascular disruption AOP. The 25th percentile AC50 values showed activity relevant to vascular regulation, such as endothelial cell-related signaling (ER1 transactivation, decreased P-selectin) and inflammatory cytokine signals (MCP1, IL8); however, the most potent assay hits were related to estrogen receptor steroid hormone activity and cell growth regulation. While these hits could be related to a microtubule stabilization mechanism mentioned earlier [36], p53 has also been shown to have anti-angiogenic properties and PI3K isoforms have involvement in vascular physiology and disease [76]. Furthermore, estrogen receptor-mediated transcriptional modulation is well known to affect vascular effects given its association with the endothelial plasma membrane [77]. Hence, more research is needed to clarify the role of vascular versus non-vascular related mechanisms influencing 5HPP-33's observed effects on development.

For TNP-470, the ToxCast HTS assay coverage for this substance's mode of action may be incomplete as there were few ToxCast assay/assay endpoints capable of more specifically mirroring TNP-470's nanomolar potency as seen in the non-ToxCast functional assays. The ToxCast assays showing similar potency included the Tanguay Zebrafish assay and two proliferation assay endpoints. However, cell types related to vascular regulation were represented in the 25th percentile AC50 values, including assay endpoints related to cellular regulation (cell proliferation), endothelial cell-related signaling (decreased P-selectin), tissue matrix remodeling (Collagen III), and inflammatory cytokine signals (NFkB, M-CSF, IL8). Furthermore, a linkage between non-canonical Wnt signaling (shown above to be affected through TNP-470's primary mechanism of action) and angiogenesis was previously reported [78]. Alternatively, the developmental toxicity of TNP-470 may be less related to a vascular MoA as other zebrafish research has shown anti-angiogenic activity of TNP-470 initiating at 100 μM [27], well above the adverse developmental effect concentration in our study.

Research aimed at clarifying the causality of vascular disruption with the observed developmental effects in cultured embryos with 5HPP-33 and TNP-470 is currently underway. Use of cultured embryos allows for the complex developmental processes to progress in the conceptual unit (embryo + early placenta) while affording a targeted mechanistic evaluation without the overlaid influence of the maternal physiological system.

5.0 Summary and Conclusion

Recent use of HTS assays in toxicity hazard evaluations, such as in the US EPA's ToxCast and the multi-agency Tox21 programs, provides new opportunities to develop and evaluate adverse outcome pathways (AOPs). Linking specific HTS assay responses to *in vivo* adverse outcomes remains a limitation with these approaches. Use of HTS assays in a tiered testing paradigm with more complex functional *in vitro* assays as a second tier is a valuable approach in prioritization of necessary *in vivo* toxicity testing. Focusing on embryonic vascular disruption as a prototypical pathway we showed in this proof of concept that HTS assays can be useful as a first tier approach to identify molecular initiating events and other key cellular events; however, inclusion of more complex functional *in vitro* assays provide a valuable intermediate testing tier whereby the predictivity of HTS data may be informed. Integration of zebrafish embryo development assays into ToxCast has shown benefit in the current research. One powerful application of the second tier data will be use of phenotypic response information from these complex assays to evaluate outputs from cell-agent based machine learning computer models based on HTS data, such as the one recently created for blood vessel development [15]. The combination of HTS assays with complex functional *in vitro* assays will provide additional mechanistic data and aid in the interpretation of HTS assays for the purposes of prioritizing *in vivo* testing. This approach, while useful for all toxicity types, holds particular importance for the evaluation of embryo/fetal development given the significance of this hazard type and its inherent complexity.

Supplementary Material

Refer to Web version on PubMed Central for supplementary material.

Acknowledgments

This work was sponsored through Strategic Research Project (SRP) funding at The Dow Chemical Company. Collaboration with the U.S. Environmental Protection Agency was made possible by joint agreement to the work product scope. The authors gratefully acknowledge the support of V.A. Marshall, A.J. Wood, L.K. Sosinski, D. DeLine in the conduct of this work.

References

1. Chung AS and Ferrara N, Developmental and pathological angiogenesis. Annu Rev Cell Dev Biol, 2011 27: p. 563–84. [PubMed: 21756109]
2. Husain T, et al., Descriptive epidemiologic features shared by birth defects thought to be related to vascular disruption in Texas, 1996–2002. Birth Defects Res A Clin Mol Teratol, 2008 82(6): p. 435–40. [PubMed: 18383510]
3. Shalaby F, et al., Failure of blood-island formation and vasculogenesis in Flk-1-deficient mice. Nature, 1995 376(6535): p. 62–6. [PubMed: 7596435]

4. Cerdeira AS and Karumanchi SA, Angiogenic factors in preeclampsia and related disorders. Cold Spring Harb Perspect Med, 2012 2(11).
5. Rutland CS, et al., Maternal administration of anti-angiogenic agents, TNP-470 and Angiostatin4.5, induces fetal microphthalmia. Mol Vis, 2009 15: p. 1260–9. [PubMed: 19572040]
6. D'Amato RJ, et al., Thalidomide is an inhibitor of angiogenesis. Proc Natl Acad Sci U S A, 1994 91(9): p. 4082–5. [PubMed: 7513432]
7. van Gelder MM, et al., Teratogenic mechanisms of medical drugs. Hum Reprod Update, 2010 16(4): p. 378–94. [PubMed: 20061329]
8. Gold NB, Westgate MN, and Holmes LB, Anatomic and etiological classification of congenital limb deficiencies. Am J Med Genet A, 2011 155A(6): p. 1225–35. [PubMed: 21557466]
9. Therapontos C, et al., Thalidomide induces limb defects by preventing angiogenic outgrowth during early limb formation. Proc Natl Acad Sci U S A, 2009 106(21): p. 8573–8. [PubMed: 19433787]
10. Kleinstreuer NC, et al., Environmental impact on vascular development predicted by high-throughput screening. Environ Health Perspect, 2011 119(11): p. 1596–603. [PubMed: 21788198]
11. Knudsen TB and Kleinstreuer NC, Disruption of embryonic vascular development in predictive toxicology. Birth Defects Res C Embryo Today, 2011 93(4): p. 312–23. [PubMed: 22271680]
12. Kavlock R, et al., Update on EPA's ToxCast program: providing high throughput decision support tools for chemical risk management. Chem Res Toxicol, 2012 25(7): p. 1287–302. [PubMed: 22519603]
13. Birnbaum LS, My Winding Road: From Microbiology to Toxicology and Environmental Health. Annu Rev Pharmacol Toxicol, 2016 56: p. 1–17. [PubMed: 26514198]
14. Sipes NS, et al., Predictive models of prenatal developmental toxicity from ToxCast high-throughput screening data. Toxicol Sci, 2011 124(1): p. 109–27. [PubMed: 21873373]
15. Kleinstreuer N, et al., A computational model predicting disruption of blood vessel development. PLoS Comput Biol, 2013 9(4): p. e1002996. [PubMed: 23592958]
16. Berridge BR, et al., Technological Advances in Cardiovascular Safety Assessment Decrease Preclinical Animal Use and Improve Clinical Relevance. ILAR J, 2016 57(2): p. 120–132. [PubMed: 28053066]
17. Atienzar FA, et al., Predictivity of dog co-culture model, primary human hepatocytes and HepG2 cells for the detection of hepatotoxic drugs in humans. Toxicol Appl Pharmacol, 2014 275(1): p. 44–61. [PubMed: 24333257]
18. Staton CA, Reed MW, and Brown NJ, A critical analysis of current in vitro and in vivo angiogenesis assays. Int J Exp Pathol, 2009 90(3): p. 195–221. [PubMed: 19563606]
19. Ellis-Hutchings RG and Carney EW, Whole embryo culture: a "New" technique that enabled decades of mechanistic discoveries. Birth Defects Res B Dev Reprod Toxicol, 2010 89(4): p. 304–12. [PubMed: 20803690]
20. Panzica-Kelly JM, et al., Morphological score assignment guidelines for the dechorionated zebrafish teratogenicity assay. Birth Defects Res B Dev Reprod Toxicol, 2010 89(5): p. 382–95. [PubMed: 20836125]
21. Wilson V and Beddington RS, Cell fate and morphogenetic movement in the late mouse primitive streak. Mech Dev, 1996 55(1): p. 79–89. [PubMed: 8734501]
22. Fleming A, et al., Mechanisms of normal and abnormal neurulation: evidence from embryo culture studies. Int J Dev Biol, 1997 41(2): p. 199–212. [PubMed: 9184327]
23. Foerst-Potts L and Sadler TW, Disruption of Msx-1 and Msx-2 reveals roles for these genes in craniofacial, eye, and axial development. Dev Dyn, 1997 209(1): p. 70–84. [PubMed: 9142497]
24. Osumi-Yamashita N, Ninomiya Y, and Eto K, Mammalian craniofacial embryology in vitro. Int J Dev Biol, 1997 41(2): p. 187–94. [PubMed: 9184325]
25. Nakagawa M, et al., Analysis of heart development in cultured rat embryos. J Mol Cell Cardiol, 1997 29(1): p. 369–79. [PubMed: 9040051]
26. Ellis-Hutchings RG, et al., In Vitro Screening Methods for Developmental Toxicology., in Developmental and Reproductive Toxicology, a Practical Approach., 3rd edition., Hood R, Editor. 2011, Taylor and Francis.

27. Chimote G, et al., Comparison of effects of anti-angiogenic agents in the zebrafish efficacy-toxicity model for translational anti-angiogenic drug discovery. Drug Des Devel Ther, 2014 8: p. 1107–23.
28. Stainier DY and Fishman MC, The zebrafish as a model system to study cardiovascular development. Trends Cardiovasc Med, 1994 4(5): p. 207–12. [PubMed: 21244869]
29. Bohnsack BL, et al., Signaling hierarchy downstream of retinoic acid that independently regulates vascular remodeling and endothelial cell proliferation. Genes Dev, 2004 18(11): p. 1345–58. [PubMed: 15175265]
30. Jojovic M, Wolf F, and Mangold U, Epidermal growth factor, vascular endothelial growth factor and progesterone promote placental development in rat whole-embryo culture. Anat Embryol (Berl), 1998 198(2): p. 133–9. [PubMed: 9725772]
31. Nagase T, et al., Hedgehog signalling in vascular development. Angiogenesis, 2008 11(1): p. 71–7. [PubMed: 18301996]
32. Noguchi T, et al., Angiogenesis inhibitors derived from thalidomide. Bioorg Med Chem Lett, 2005 15(24): p. 5509–13. [PubMed: 16183272]
33. Newman CG, The thalidomide syndrome: risks of exposure and spectrum of malformations. Clin Perinatol, 1986 13(3): p. 555–73. [PubMed: 3533365]
34. Kizaki M and Hashimoto Y, New tubulin polymerization inhibitor derived from thalidomide: implications for anti-myeloma therapy. Curr Med Chem, 2008 15(8): p. 754–65. [PubMed: 18393844]
35. Li PK, et al., A thalidomide analogue with in vitro antiproliferative, antimitotic, and microtubule-stabilizing activities. Mol Cancer Ther, 2006 5(2): p. 450–6. [PubMed: 16505120]
36. Rashid A, et al., Thalidomide (5HPP-33) suppresses microtubule dynamics and depolymerizes the microtubule network by binding at the vinblastine binding site on tubulin. Biochemistry, 2015 54(12): p. 2149–59. [PubMed: 25747795]
37. Iguchi T, et al., Novel tubulin-polymerization inhibitor derived from thalidomide directly induces apoptosis in human multiple myeloma cells: possible anti-myeloma mechanism of thalidomide. Int J Mol Med, 2008 21(2): p. 163–8. [PubMed: 18204782]
38. Shimura M, et al., Novel compound SK-1009 suppresses interleukin-6 expression through modulation of activation of nuclear factor-kappaB pathway. Biol Pharm Bull, 2012 35(12): p. 2186–91. [PubMed: 23018603]
39. Logothetis CJ, et al., Phase I trial of the angiogenesis inhibitor TNP-470 for progressive androgen-independent prostate cancer. Clin Cancer Res, 2001 7(5): p. 1198–203. [PubMed: 11350884]
40. Cline EI, et al., Prediction of in vivo synergistic activity of antiangiogenic compounds by gene expression profiling. Cancer Res, 2002 62(24): p. 7143–8. [PubMed: 12499246]
41. Klauber N, et al., Critical components of the female reproductive pathway are suppressed by the angiogenesis inhibitor AGM-1470. Nat Med, 1997 3(4): p. 443–6. [PubMed: 9095179]
42. Vetro JA, Dummitt B, and Chang Y-H, Methionine Aminopeptidase, in Aminopeptidases in Biology and Disease, Lendeckel H.a., Editor. 2004, Kluwer Academic/Plenum Publishers: New York p. 17–44.
43. Yeh JR, et al., Targeted gene disruption of methionine aminopeptidase 2 results in an embryonic gastrulation defect and endothelial cell growth arrest. Proc Natl Acad Sci U S A, 2006 103(27): p. 10379–84. [PubMed: 16790550]
44. McCollum CW, et al., Identification of vascular disruptor compounds by analysis in zebrafish embryos and mouse embryonic endothelial cells. Reproductive Toxicology 2016 pii/S0890623816304014.
45. Knudsen TB, T. T, Sarkanen R, Spencer RS, Baker NC, Franzosa JA, Tal T, Kleinstreuer NC, Cai BB, Berg EL and Heinonen T, ToxCast Model-Based Prediction of Human Vascular Disruption: correlation to endothelial tubulogenesis assays and computer simulation.. in preparation.
46. Franzosa JA, Settivari RS, Ellis-Hutchings, Kleinstreuer NC, Houck KA, Carney EW and Knudsen TB RNA-Seq analysis of the functional-link between vascular disruption and adverse developmental consequences. Reprod Toxicol in preparation.
47. Attene-Ramos MS, et al., The Tox21 robotic platform for the assessment of environmental chemicals--from vision to reality. Drug Discov Today, 2013 18(15–16): p. 716–23. [PubMed: 23732176]

48. Judson R, et al., Analysis of the Effects of Cell Stress and Cytotoxicity on In Vitro Assay Activity Across a Diverse Chemical and Assay Space. Toxicol Sci, 2016.
49. Tal T, K. C, Smith A, LaLone C, Kennedy B, Tennant A, McCollum C, Bondesson M, Knudsen T, Padilla S and Kleinstreuer N Screening for chemical vascular disruptors in zebrafish to evaluate a predictive model for developmental vascular toxicity. Reprod Toxicol, in press.
50. Cockroft D, Dissection and culture of postimplantation embryos, in Postimplantation culture of mammalian embryos-a practical approach, Copp A and Cockroft D, Editors. 1990, Oxford University Press: Oxford p. 15–40.
51. Daston GP, et al., Difference in teratogenic potency of ethylenethiourea in rats and mice: relative contribution of embryonic and maternal factors. Teratology, 1989 40(6): p. 555–66. [PubMed: 2623643]
52. Brown NA and Fabro S, Quantitation of rat embryonic development in vitro: a morphological scoring system. Teratology, 1981 24(1): p. 65–78. [PubMed: 7302873]
53. Lowry OH, et al., Protein measurement with the Folin phenol reagent. J Biol Chem, 1951 193(1): p. 265–75. [PubMed: 14907713]
54. Westerfield M, The Zebrafish Book: A guide for the laboratory use of zebrafish (Danio rerio). 5th ed. 2007, Eugene, OR: University of Oregon Press.
55. Abassi YA, et al., Kinetic cell-based morphological screening: prediction of mechanism of compound action and off-target effects. Chem Biol, 2009 16(7): p. 712–23. [PubMed: 19635408]
56. Kimmel CB, et al., Stages of embryonic development of the zebrafish. Dev Dyn, 1995 203(3): p. 253–310. [PubMed: 8589427]
57. OECD, Test No. 236: Fish Embryo Acute Toxicity (FET) Test. 2013, OECD Publishing.
58. Gustafson AL, et al., Inter-laboratory assessment of a harmonized zebrafish developmental toxicology assay - progress report on phase I. Reprod Toxicol, 2012 33(2): p. 155–64. [PubMed: 22210281]
59. Selderslaghs IW, Blust R, and Witters HE, Feasibility study of the zebrafish assay as an alternative method to screen for developmental toxicity and embryotoxicity using a training set of 27 compounds. Reprod Toxicol, 2012 33(2): p. 142–54. [PubMed: 21871558]
60. Motulsky HJ and Christopoulos A, Fitting models to biological data using linear and nonlinear regression: a practical guide to curve fitting, in GraphPad Software, Inc. 2003, Oxford University Press: San Diego, CA.
61. Franzosa J, et al., RNA-Seq Analysis of the Functional Link Between Vascular Disruption and Adverse Developmental Consequences. The Toxicologist, Supplement to Toxicological Sciences, 2014: p. 456.
62. Kleinstreuer NC, et al., Phenotypic screening of the ToxCast chemical library to classify toxic and therapeutic mechanisms. Nat Biotechnol, 2014 32(6): p. 583–91. [PubMed: 24837663]
63. Houck KA, et al., Profiling bioactivity of the ToxCast chemical library using BioMAP primary human cell systems. J Biomol Screen, 2009 14(9): p. 1054–66. [PubMed: 19773588]
64. Vichai V and Kirtikara K, Sulforhodamine B colorimetric assay for cytotoxicity screening. Nat Protoc, 2006 1(3): p. 1112–6. [PubMed: 17406391]
65. Lee CJ, et al., Fluorothalidomide: a characterization of maternal and developmental toxicity in rabbits and mice. Toxicol Sci, 2011 122(1): p. 157–69. [PubMed: 21505091]
66. Beedie SL, et al., In vivo screening and discovery of novel candidate thalidomide analogs in the zebrafish embryo and chicken embryo model systems. Oncotarget, 2016.
67. Padilla S, et al., Zebrafish developmental screening of the ToxCast Phase I chemical library. Reprod Toxicol, 2012 33(2): p. 174–87. [PubMed: 22182468]
68. Truong L, et al., Multidimensional in vivo hazard assessment using zebrafish. Toxicol Sci, 2014 137(1): p. 212–33. [PubMed: 24136191]
69. Didcock K, Jackson D, and Robson JM, The action of some nucleotoxic substances on pregnancy. Br J Pharmacol Chemother, 1956 11(4): p. 437–41. [PubMed: 13383124]
70. Prakash V and Timasheff SN, Aging of tubulin at neutral pH: stabilization by colchicine and its analogues. Arch Biochem Biophys, 1992 295(1): p. 146–52. [PubMed: 1575511]

71. Luo J, et al., Placental abnormalities in mouse embryos lacking the orphan nuclear receptor ERR-beta. Nature, 1997 388(6644): p. 778–82. [PubMed: 9285590]
72. Latos PA, et al., Fgf and Esrrb integrate epigenetic and transcriptional networks that regulate self-renewal of trophoblast stem cells. Nat Commun, 2015 6: p. 7776. [PubMed: 26206133]
73. Marlow F, et al., No tail co-operates with non-canonical Wnt signaling to regulate posterior body morphogenesis in zebrafish. Development, 2004 131(1): p. 203–16. [PubMed: 14660439]
74. Yamaguchi TP, et al., A Wnt5a pathway underlies outgrowth of multiple structures in the vertebrate embryo. Development, 1999 126(6): p. 1211–23. [PubMed: 10021340]
75. Ma AC, et al., Methionine aminopeptidase 2 is required for HSC initiation and proliferation. Blood, 2011 118(20): p. 5448–57. [PubMed: 21937698]
76. Morello F, et al., LXR-activating oxysterols induce the expression of inflammatory markers in endothelial cells through LXR-independent mechanisms. Atherosclerosis, 2009 207(1): p. 38–44. [PubMed: 19426978]
77. Kim KH, Young BD, and Bender JR, Endothelial estrogen receptor isoforms and cardiovascular disease. Mol Cell Endocrinol, 2014 389(1–2): p. 65–70. [PubMed: 24530925]
78. Stefater JA 3rd, et al., Regulation of angiogenesis by a non-canonical Wnt-Flt1 pathway in myeloid cells. Nature, 2011 474(7352): p. 511–5. [PubMed: 21623369]

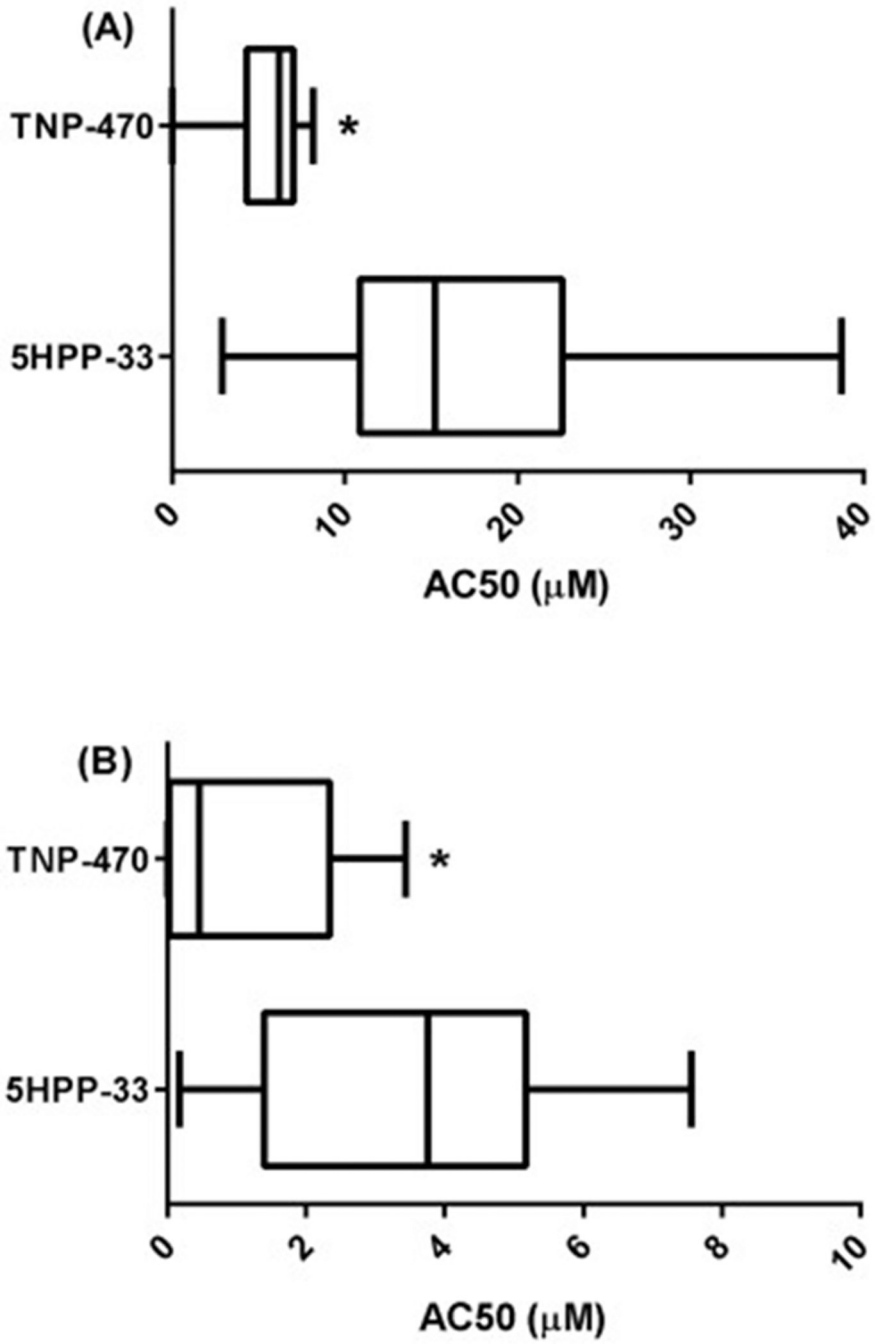

Fig. 1.

Box and whisker plot of (A) ToxCast BioSeek AC50 Values, (B) ToxCast lowest 25th Percentile AC50 Values. Line in the middle of the box is plotted at the median and the box extends from the 25th to 75th percentiles. The whiskers go down to the smallest value and up to the largest. * Statistically lower than the 5HP3 group via t-test at $P < 0.05$.

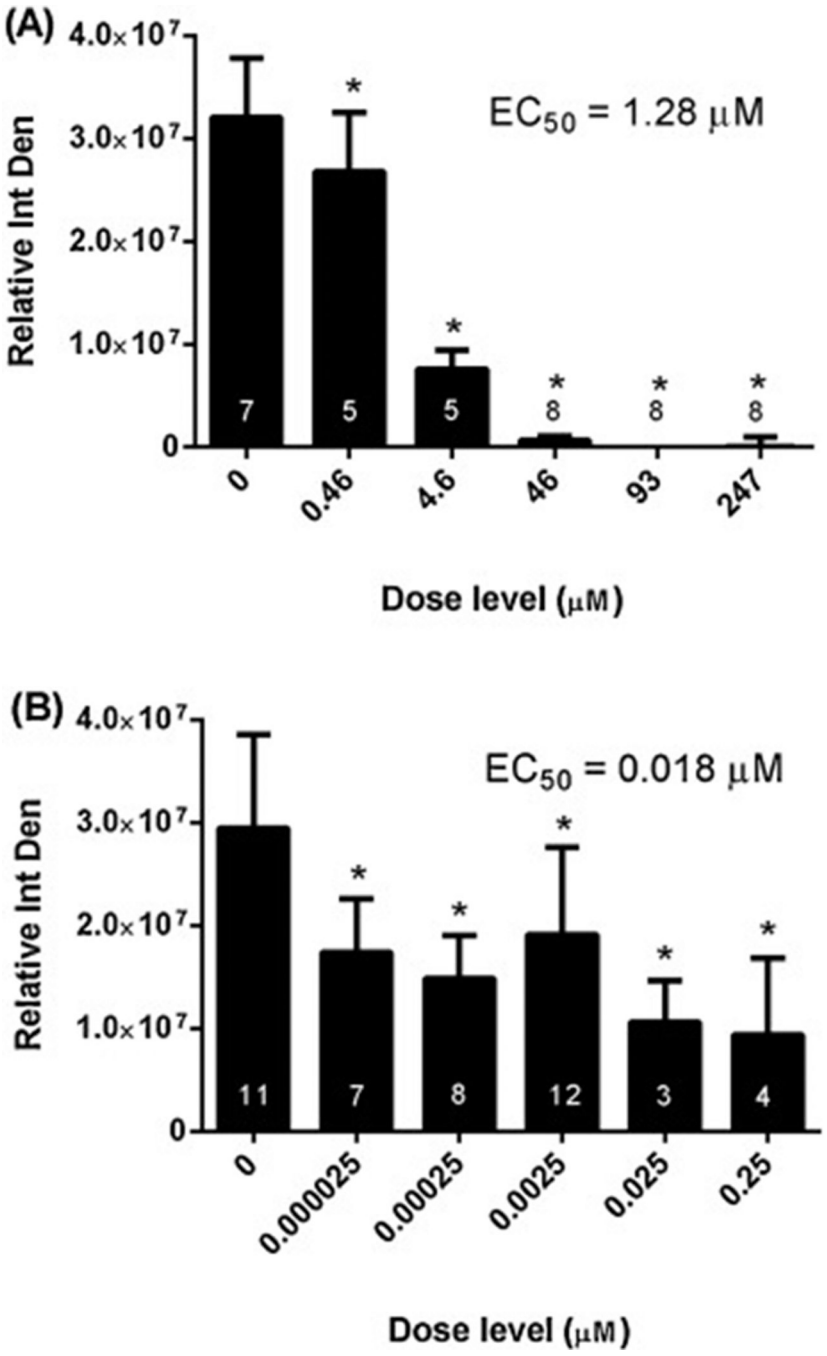

Fig. 2.

Microvessel Outgrowth Inhibition Dose-response. Rat aortic explants were incubated in the absence or presence of increasing concentrations of (A) 5HPP-33 or (B) TNP-470 for four days followed by image acquisition and outgrowth quantification. Integrated density values of the microvessel outgrowth were normalized to the values at the beginning of treatment. Data are expressed as the mean relative (normalized) integrated density ± SD. Samples sizes are shown in the respective figures. Nonlinear regression analysis was used to estimate the concentration that inhibited 50% of the microvessel outgrowth relative to the untreated

explants (EC50) using nonlinear curve fitting software. * Statistically different from the untreated group via 1-way ANOVA with Dunnett's Multiple Comparison Test at $P < 0.05$.

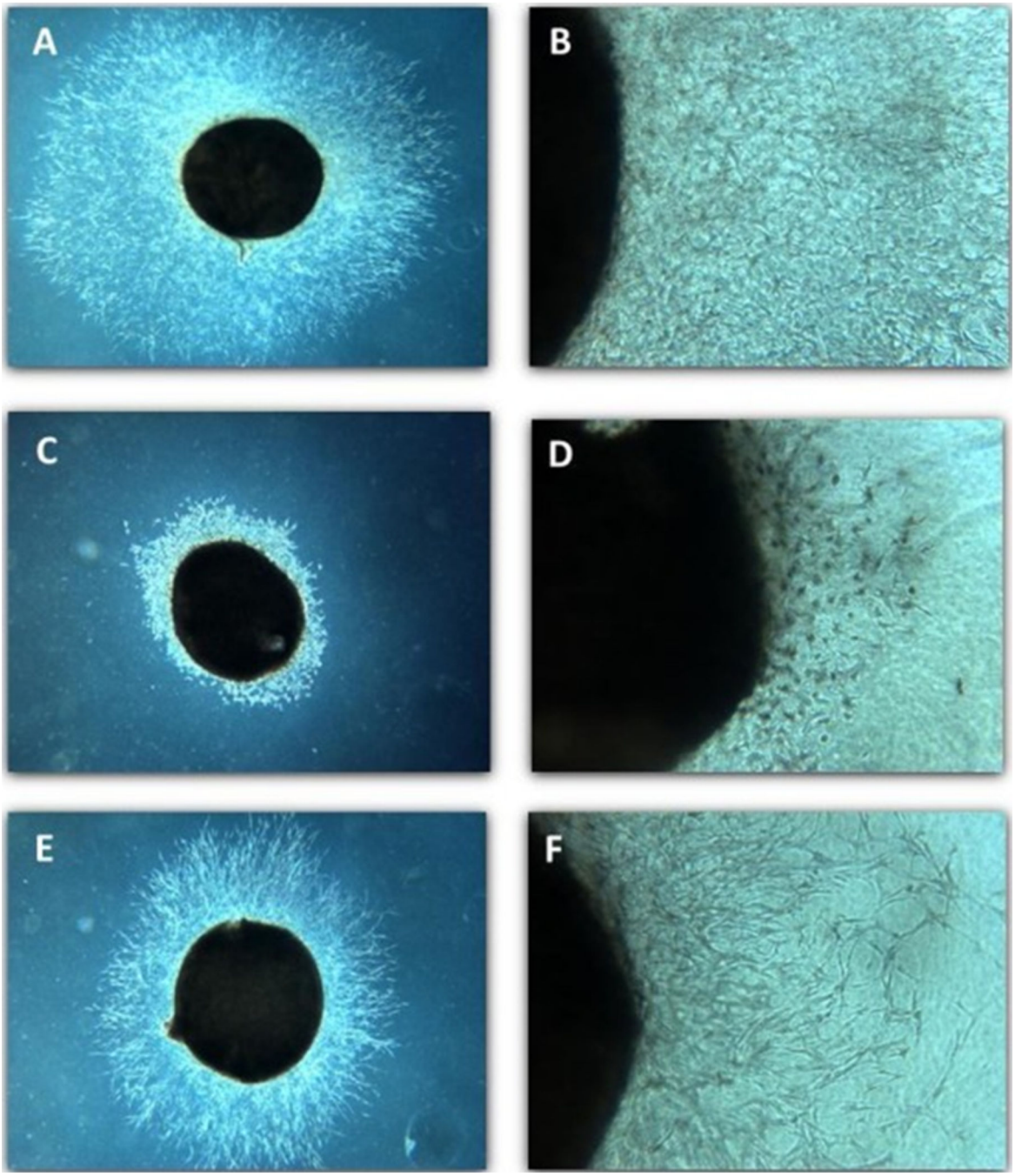

Fig. 3.

Photomicrographs of Microvessel Outgrowth Inhibition. Images of representative rat aortic explants following four days of treatment (test day 8). Untreated control (A, B), 5HPP-33 (46 μM; C, D), and TNP-470 (0.0025 μM; E, F). Magnification = 20 × (A, C, E) or 100 × (B, D, F). The explant is visible as the dark circle while microvessel outgrowth can be seen extending out from the explant.

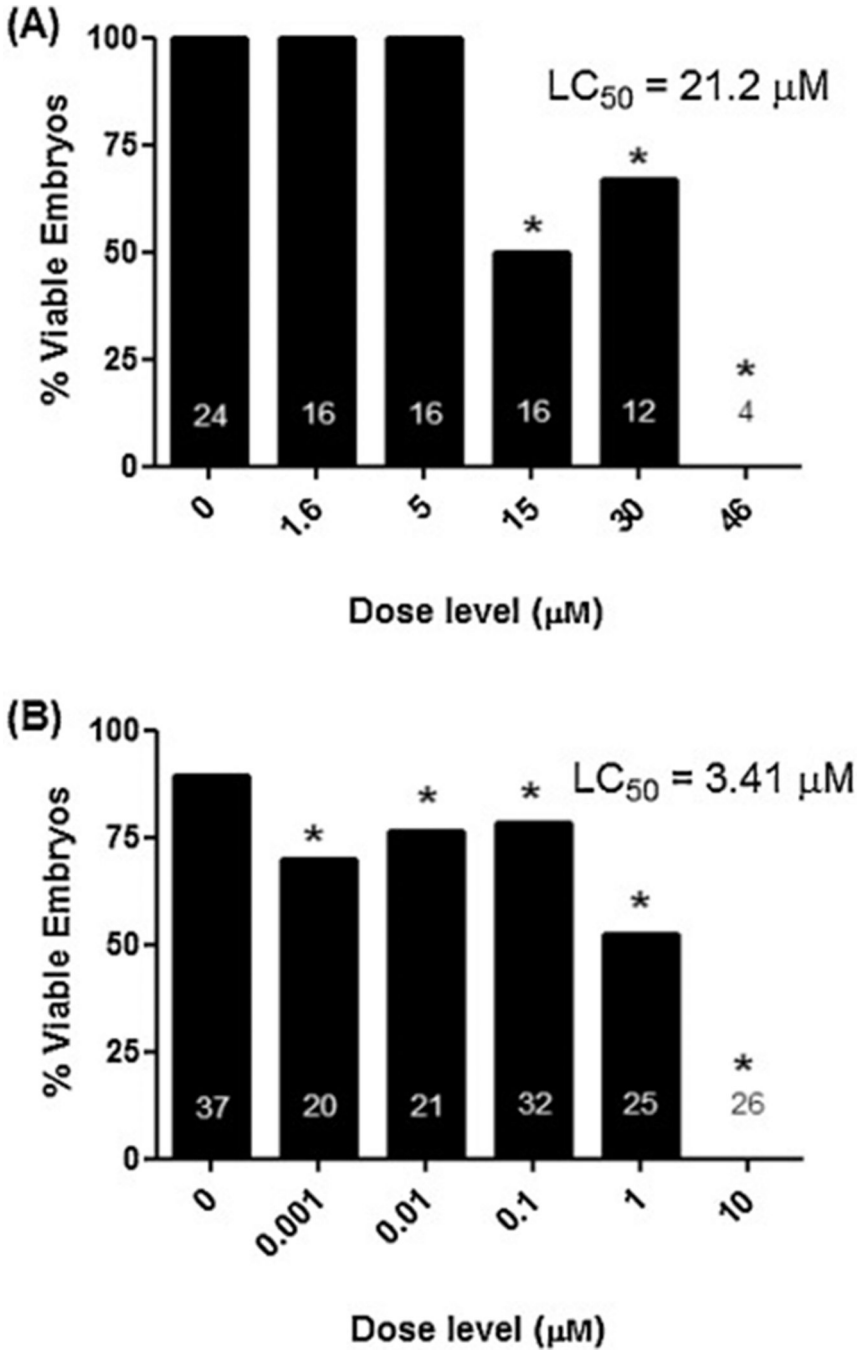

Fig. 4.

Reductions in Embryo Viability following 5HPP-33 Exposure. (A) Rat Whole Embryo Culture. (B) Zebrafish Embryotoxicity Test. Gestation day (GD) 10 rat embryos and 1–4 h post fertilization (hpf) zebrafish embryos were cultured under static conditions in the absence or presence of increasing concentrations of 5HPP-33 for two or five days, respectively, followed by evaluation of viability and morphology. 5HPP-33 exposure primarily resulted in reductions in mean% embryo viability. Samples sizes are shown in the respective figures. Nonlinear regression analysis was used to estimate the concentration

lethal to 50% of the embryo (LC50) using nonlinear curve fitting software. * Statistically different from the untreated group via 1-way ANOVA with Dunnett's Multiple Comparison Test at $P < 0.05$.

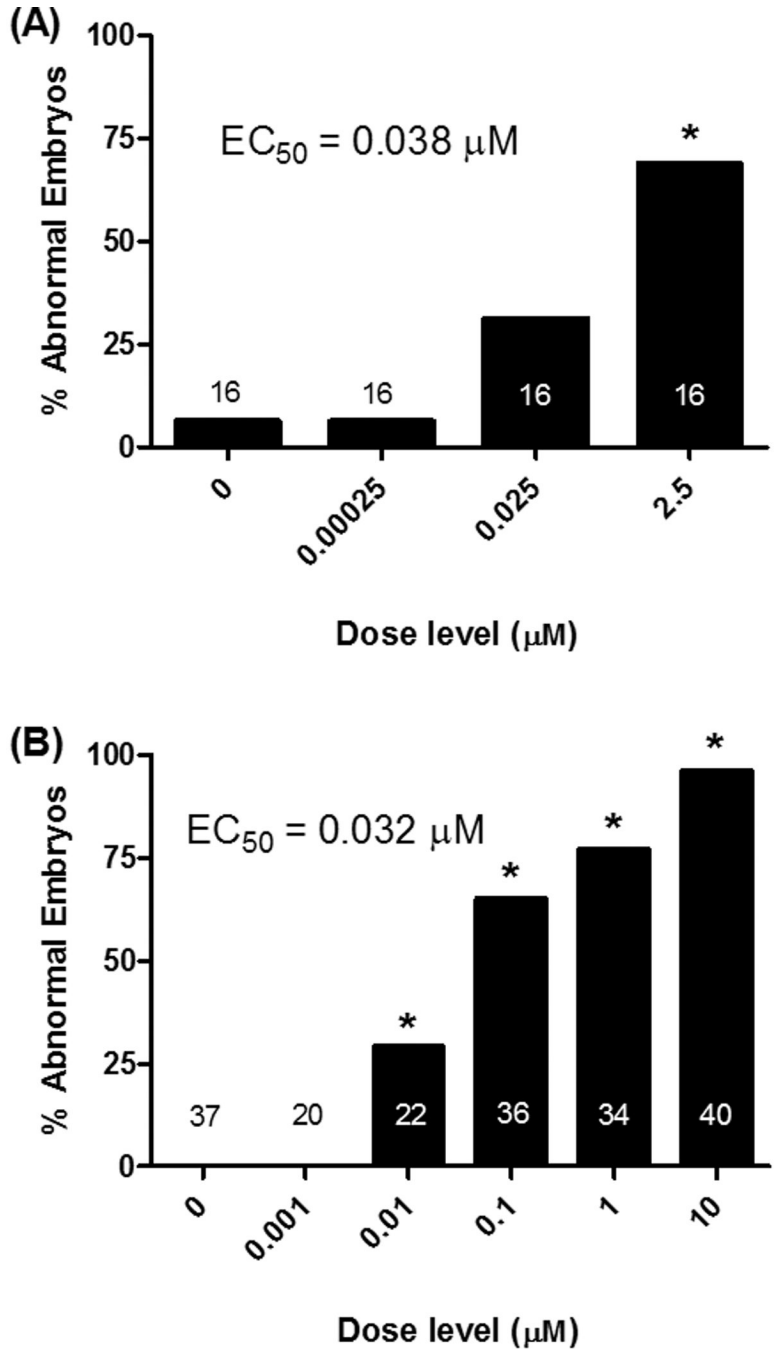

Figure 5. Dose-dependent Embryo Dysmorphology following TNP-470 Exposure.

(A) Rat Whole Embryo Culture. (B) Zebrafish Embryotoxicity Test. Gestation day (GD) 10 rat embryos and 1–4 hours post fertilization (hpf) zebrafish embryos were cultured under static conditions in the absence or presence of increasing concentrations of TNP-470 for two or five days, respectively, followed by evaluation of viability and morphology. A total of 18 or 12 separate structural features were evaluated in WEC and ZET, respectively (see methods for more details). TNP-470 exposure resulted in developmental abnormalities in the absences of lethality. The mean % of abnormal embryos is shown along with the samples

sizes in the respective figures. Nonlinear regression analysis was used to estimate the concentration that caused a 50% incidence of abnormal embryos (EC50) using nonlinear curve fitting software. * Statistically different from the untreated group via 1-way ANOVA with Dunnett's Multiple Comparison Test at $P < 0.05$.

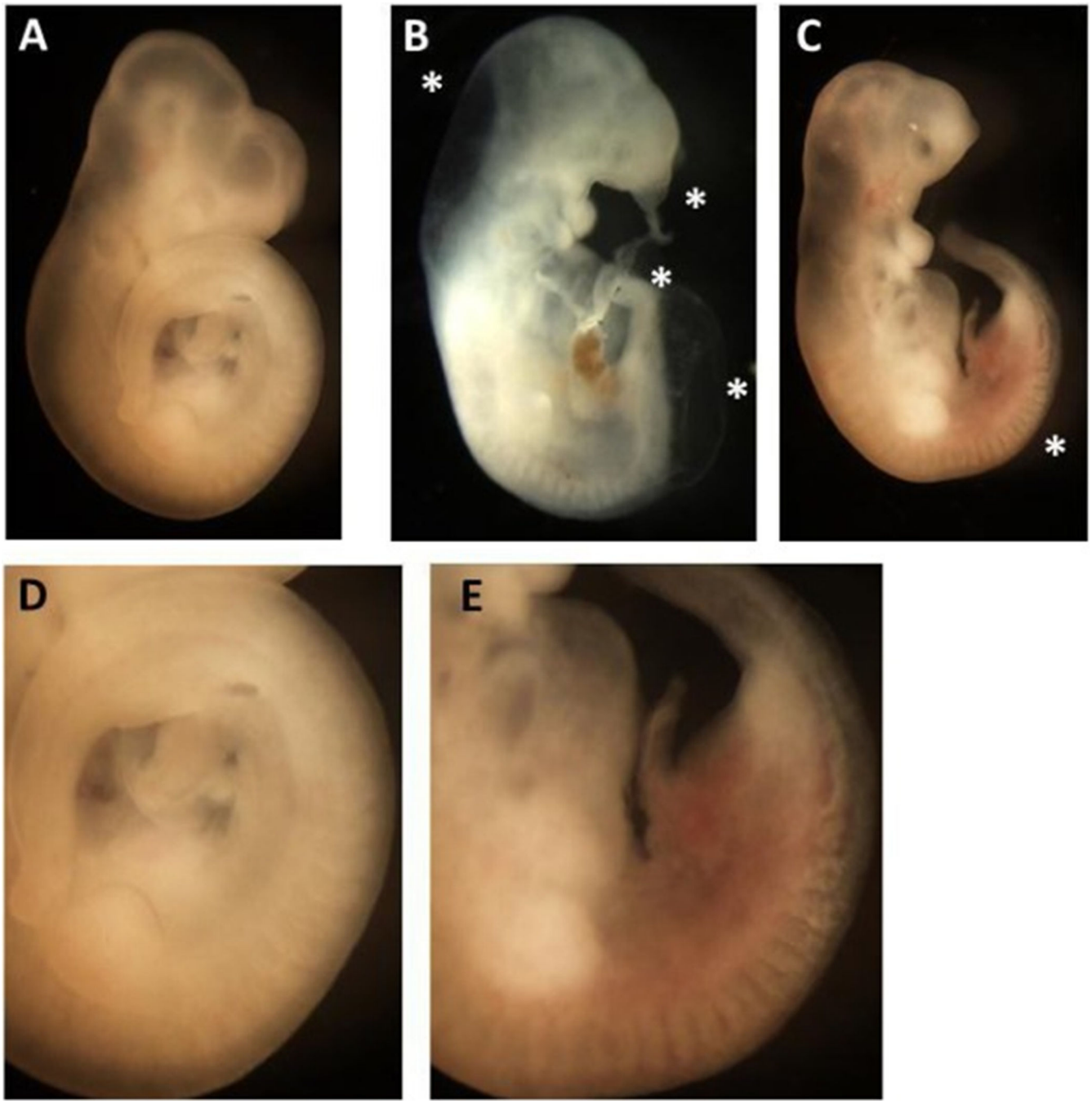

Fig. 6.

TNP-470-induced Embryo Dysmorphology in Rat WEC (Representative photomicrographs). Photomicrographs of representative rat embryos following two days of culture in the absence or presence of increasing concentrations of TNP-470. Untreated control (A, D), TNP-470 (2.5 μM; B, C, E). Magnification = 20× (A,B, and C) or 50× (D, E). TNP-470 was teratogenic causing primarily caudal extension defects and abnormal somite patterning. The asterisks in 6 B refer to reduced caudal length and kinking, blisters in the caudal and fronto-nasal process, and distended hindbrain. The asterisks in 6C refers to the somite region most

affected in TNP-470-exposed embryo. Figs. 6D and E show higher magnification of this region where reductions in somite size, definition and altered shape are apparent with TNP-470 exposure (6E) compared to untreated embryos (6D).

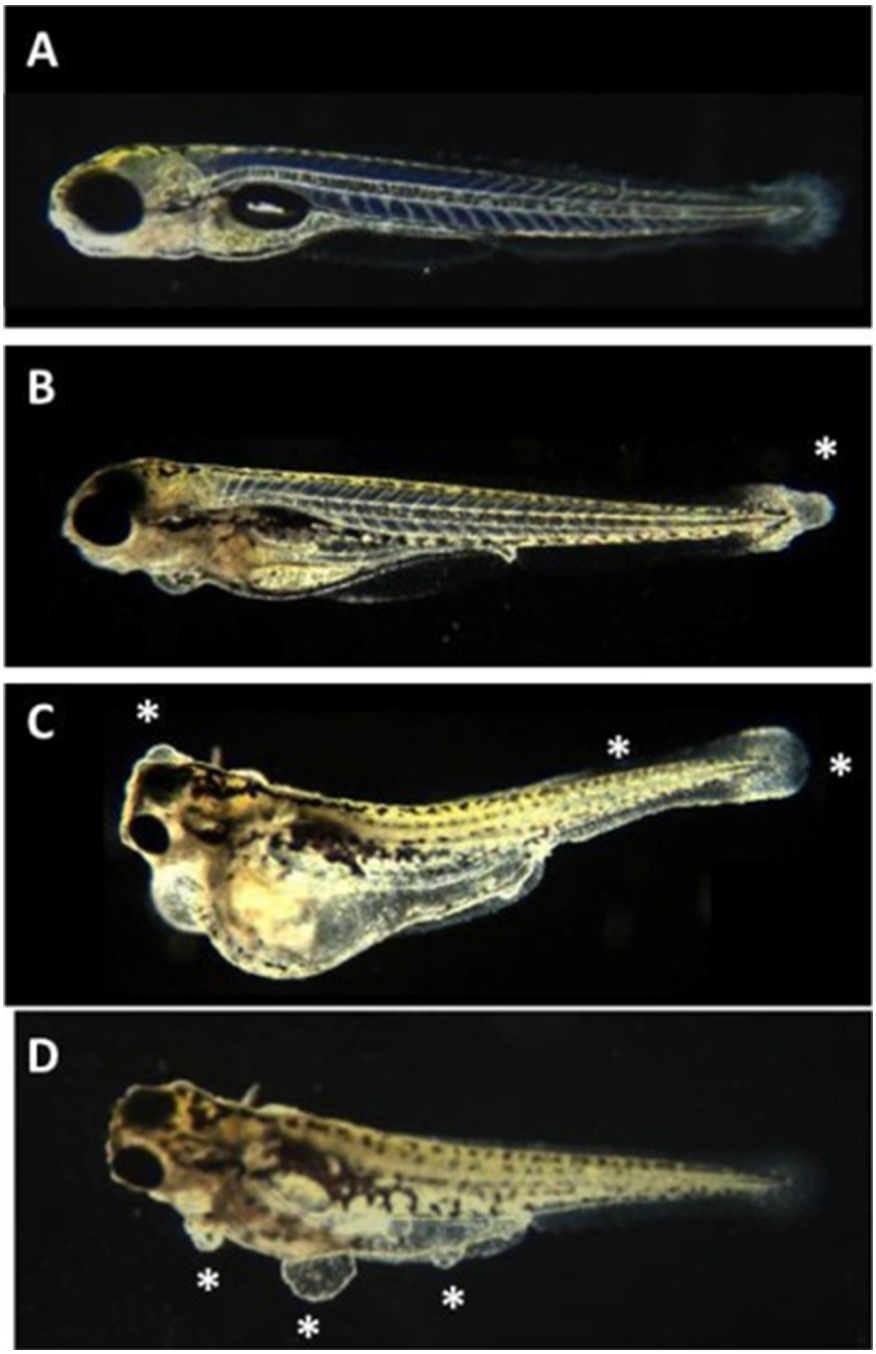

Fig. 7.

TNP-470-induced Zebrafish Embryo Dysmorphology (Representative photomicrographs). Photomicrographs of representative zebrafish embryos following five days of culture in the absence or presence of increasing concentrations of TNP-470. Magnification = 100×. Untreated control (A), TNP-470 (7B, 0.1 μM; 7C, 10 μM; 7D, 1 μM). TNP-470 was teratogenic causing primarily caudal defects and abnormal somite patterning. The asterisks

in 7 B shows tail fin abnormalities; in 7C shows tail fin abnormalities, disorganized somites, and forebrain blisters; in 7D shows blisters.

Table 1.

Functional and ToxCast HTS Assay Characteristics.

Assay Platform	Species	Description	Test concentrations 5HPP-33 (μM)	Test concentrations TNP-470 (μM)
Functional *In Vitro*				
Whole Embryo Culture (WEC)	Rat	Whole organism	1.6–46.0	0.00025–2.5
Fish Embryotoxicity (ZET)	Zebrafish	Whole organism-chorion on	0.001–10.0	0.001–10.0
Aortic Explant Assay (AEA)	Rat	Primary organ culture	0.46–247	0.000025–0.25
ToxCast *In Vitro* HTS				
ACEA Biosciences (ACEA)	Human	Real-time electronic sensing for cytotoxicity and estrogen-dependent growth in T-47D cells[a]	0.006–100	NA
Apredica (APR)	Human	High-content cellular imaging HepG2 cells[b]	0.39–200	0.39–200
Attagene (ATG)	Human	Multiplexed transcriptional reporter genes in HepG2 cells[c]	0.09–200	0.09–200
BioSeek (BSK)	Human	Multiplexed protein expression profiling (BioMap) in primary human cell (co)cultures[d]	1.48–40	1.48–40
CeeTox	Human	Multiplexed enzyme activity for steroids in H295R cells[e]	0.4–100	NA
NCCT	Rat, pig	TPO inhibition assays in a cell-free format[f]	NA	0.03–30
NHEERL ZF	Zebrafish	Whole organism-chorion on[g]	0.03–80	0.009–30
Novascreen (NVS)	Human, rat, bovine, guinea pig, sheep, mouse, rabbit, boar	Receptor-binding and enzyme activity assays (ENZ) in a cell-free format[h]	0.009–20 0.02–50 (ENZ)	0.009–20 0.02–50 (ENZ)
Odyssey Thera (OT)	Human	Protein-fragment complementation technology targeting signaling pathways in cells[i]	0.3–100	0.3–100
Tanguay ZF	Zebrafish	Whole organism- dechorionated [j]	0.006–60	0.002–20
Tox21 (Tox21)	Human	Cellular assays targeting nuclear receptors, cell stress pathways and cell viability[k]	0.001–100	0.0002–30

Table 2.

ToxCast *in vitro* HTS Assay Findings.

Source	**Total Assay Endpoints**		**Number of Active Assay Endpoints (% of Source)**		**Number Active in the 25th Percentile AC50 values (% of Source)**	
	5HPP-33	**TNP-470**	**5HPP-33**	**TNP-470**	**5HPP-33**	**TNP-470**
ACEA	2	0	2 (100)	0	1 (50.0)	0
APR	39	39	17 (43.6)	0	7 (41.2)	0
Attagene	163	163	40 (24.5)	14 (8.6)	5 (12.5)	3 (21.4)
BioSeek	174	174	65 (37.4)	43 (24.7)	9 (13.8)	6 (37.5)
CeeTox	20	20	9 (45.0)	0	1 (11.1)	0
NCCT	1	4	0	1 (25.0)	0	0
NHEERL ZF	1	1	1 (100)	0	1 (100)	0
Novascreen	338	326	14 (4.4)	4 (1.2)	9 (64.3)	4 (100)
OT	17	17	6 (35.3)	1 (5.9)	5 (83.3)	0
Tanguay ZF	19	19	2 (10.5)	8 (42.1)	0	8 (100)
Tox21	113	113	47 (41.6)	11 (9.7)	9 (19.1)	1 (9.1)
Assay Summary	**Number of assays**		**Number of Active Assay Endpoints (% of Total)**		**Number Active in the 25th Percentile AC50 values (% of Total)**	
	5HPP-33	**TNP-470**	**5HPP-33**	**TNP-470**	**5HPP-33**	**TNP-470**
Totals	887	876	202 (22.8)	82 (9.4)	47(25)	21 (25)
Median AC50 ± SD (μM)	NA	NA	18.7 ± 30	6.6 ± 9.6	3.63 ± 2.2	0.45 ± 1.3

Table 3.

ToxCast *in vitro* HTS Assay Data: 25th Percentile AC50 Values

(A) 5HPP-33			
Assay Endpoint[1]	**Description**	**Endpoint Classification**	**AC50 (μM)**
ATG_ERa_TRANS_up	Increase in ER alpha transactivation in HepG2 cells	estrogen receptor alpha	0.168
TOX21_ERa_LUC_BG1_Agonist	Agonism against ER 1 in BG1 cells	estrogen receptor alpha	0.196
ATG_PXR_TRANS_up	Increase in PXR transactivation in HepG2 cells	xenosensor	0.263
OT_ERa_EREGFP_0480	Increase in ERa fluorescent protein induction in HeLa cells	estrogen receptor alpha	0.306
OT_ERa_EREGFP_0120	Increase in ERa fluorescent protein induction in HeLa cells	estrogen receptor alpha	0.317
ACEA_T47D_80hr_Positive	Effect on cell growth kinetics in T47D cells	Cell growth regulation	0.448
TOX21_ERa_BLA_Agonist_ratio	Induction of ERa beta lactamase in HEK293T cells	estrogen receptor alpha	0.520
NVS_ENZ_hPI3Ka	Inhibition of human PI3K enzyme activity (cell-free)	Cell growth regulation	0.572
NVS_NR_mERa	Cell-free binding to the mouse estrogen receptor alpha	mouse estrogen receptor liganding	0.980
Tox21_p53_BLA_ratio[2]	Activation of p53 signaling pathway in HCT116 cells	cell cycle checkpoint	1.036
NVS_NR_bER	Cell-free binding to the bovine estrogen receptor alpha	bovine estrogen receptor liganding	1.062
NVS_NR_hER	Cell-free binding to the human estrogen receptor alpha	human estrogen receptor liganding	1.337
OT_ER_ERbERb_0480	Increase in ERb fluorescent protein induction in HeLa cells	estrogen receptor	1.396
OT_ER_ERaERb_0480	Increase in ERa fluorescent protein induction in HEK293T cells	estrogen receptor	1.618
TOX21_MMP_ratio_down	Decreased membrane potential in HEPG2 cells	mitochondrial depolarization	2.518
NVS_ENZ_oCOX1	Cell-free enzymatic activity to sheep prostaglandin-endoperoxide synthase 1	cyclooxygenase-1 activity	2.770
BSK_3C_Proliferation_down	Decrease in proliferation in umbilical vein endothelial cells	Cell growth regulation	2.900
APR_HepG2_p53Act_72h_up	Activation of p53 in HepG2 cells	cell cycle checkpoint	3.074
BSK_3C_Vis_down	Decrease in visual activity in umbilical vein endothelial cells	Cellular health	3.202
ATG_ERE_CIS_up	Increase in ERS1 activation in HepG2 cells	ER steroid hormone activity	3.625
APR_HepG2_MitoticArrest_24h_up	Increase in mitochondrial arrest at 24h in HepG2 cells	Cell growth regulation	3.760
BSK_4H_MCP1_up	CCL2 upregulation in vascular umbilical vein endothelial cells	Inflammatory cytokine signals	3.765
ATG_PXRE_CIS_up	Increase in PXR activation in HepG2 cells	xenosesnor	4.064
OT_ER_ERaERa_0480	Agonism against ER 1 in HEK293T cells	ER steroid hormone activity	4.196
NVS_NR_hPXR	Inhibition of human PXR binding (cell-free)	xenosensor	4.256

(A) 5HPP-33			
Assay Endpoint[1]	**Description**	**Endpoint Classification**	**AC50 (μM)**
CEETOX_H295R_TESTO_dn	Decreased catalytic activity of testosterone in H295R cells	steroidogenesis	4.377
ATG_DR5_CIS_up	Increase in RAR cis-activation in HepG2 cells	retinoid signaling	4.386
NVS_ADME_hCYP2C9	Cell-free enzyme activity at human Cyp2C9	Detoxification/ metabolism	4.403
NHEERL_ZF_144hpf_TERATOSCORE_up	Increase in TERATOSCORE in zebrafish at 144hpf	Abnormal embryo development	4.440
BSK_3C_IL8_up	Increase in IL-8 protein levels in umbilical vein endothelial cells	Inflammatory cytokine signals	4.528
BSK_LPS_IL8_up	CXCL8 downregulation in vascular umbilical vein endothelial cell/peripheral blood mononuclear cell cocultures	Inflammatory cytokine signals	4.687
APR_HepG2_MitoMass_72h_up	Increase in mitochondrial mass in HepG2 cells	mitochondrial number	4.746
BSK_hDFCGF_TIMP1_up	Increase in TIMP metallopeptidase inhibitor protein levels in foreskin fibroblast cells	Extracellular matrix remodelling	4.754
NVS_ENZ_oCOX2	Inhibition of sheep COX2 enzymatic activity (cell-free)	cyclooxygenase-2 activity	4.911
TOX21_TR_LUC_GH3_Antagonist	Antagonism of thyroid hormone receptor alpha and beta in GH3 cells	Nuclear receptor activity	5.177
NVS_ADME_hCYP2C19	Inhibition of human CYP2C19 activity (cell-free)	Detoxification/ metabolism	5.677
APR_HepG2_CellCycleArrest_24h_dn	Decrease in cell cycle arrest at 24h in HepG2 cells	Cell growth regulation	5.946
APR_HepG2_CellCycleArrest_72h_dn	Decrease in cell cycle arrest at 72h in HepG2 cells	Cell growth regulation	6.384
BSK_4H_Pselectin_down	Decrease in P-selectin protein levels in umbilical vein endothelial cells	Endothelial cell-related signaling	6.740
APR_HepG2_StressKinase_24h_up	Increase in stress kinase enzyme activity at 24h in HepG2 cells	Cellular stress	7.050
BSK_3C_HLADR_down	Decrease in major histocompatibility complex, class II, DR alpha levels in umbilical vein endothelial cells	Immune function	7.101
APR_HepG2_MitoticArrest_72h_up	Increase in cell cycle arrest in HepG2 cells	Cell growth regulation	7.368
BSK_LPS_CD40_down	Decrease in CD40 (TNF receptor superfamily member 5) in vascular umbilical vein endothelial cell/peripheral blood mononuclear cell cocultures	Immune and inflammatory regulation	7.566

[1] Additional assay information downloadable at https://www3.epa.gov/research/COMPTOX/toxcast_assay.html

[2] Assay run multiple times (5) with consistent results (AC50 range 1.04–3.18 μM)

(B) TNP-470			
Assay Endpoint[1]	**Description**	**Endpoint Classification**	**AC50 (μM)**
BSK_3C_Proliferation_down	Decrease in proliferation in umbilical vein endothelial cells	Cell growth regulation	0.001
Tanguay_ZF_120hpf_YSE_up	Increase in yolk sac developmental defects	Abnormal embryo development	0.003
Tanguay_ZF_120hpf_PE_up	Increase in pericardial edema	Abnormal embryo development	0.009
Tanguay_ZF_120hpf_CFIN_up	Increase in caudal fin developmental defects	Abnormal embryo development	0.009
Tanguay_ZF_120hpf_AXIS_up	Increase in axial developmental defects	Abnormal embryo development	0.018
NVS_GPCR_rGHB	Increase in binding to rat tetraspanin 17 protein, important in cell adhesion, motility, activation and proliferation	G-protein coupled receptor	0.025
Tanguay_ZF_120hpf_EYE_up	Increase in eye developmental defects	Abnormal embryo development	0.034
Tanguay_ZF_120hpf_JAW_up	Increase in jaw developmental defects	Abnormal embryo development	0.040
ATG_PXRE_CIS_up	Increase in PXR activation in HepG2 cells	Xenosensor	0.323
ATG_NF_kB_CIS_dn	Decrease in NFκB activation in HepG2 cells	Immune and inflammatory regulation	0.364
Tanguay_ZF_120hpf_SNOU_up	Increase in snout developmental defects	Abnormal embryo development	0.452
ATG_IR1_CIS_dn	Decrease in 1H4 Farnesoid FXR activation in HepG2 cells	Detoxification/ metabolism	1.469
NVS_ADME_hCYP2C19	Cell-free enzyme activity at human Cyp2C19	Detoxification/ metabolism	2.032
BSK_4H_Pselectin_down	Decrease in P-selectin protein levels in umbilical vein endothelial cells	Endothelial cell-related signaling	2.048
Tanguay_ZF_120hpf_PFIN_up	Increase in pectoral fin developmental defects	Abnormal embryo development	2.189
NVS_ADME_hCYP3A4	Cell-free enzyme activity at human Cyp3A3	Detoxification/ metabolism	2.225
TOX21_ARE_BLA_agonist_ratio	Induction of beta lactamase reporter in HepG2 cells measuring transcriptional activation of ARE	Antioxidant response element	2.459
BSK_hDFCGF_CollagenIII_down	Decrease in Collagen III protein levels in foreskin fibroblast cells	Extracellular matrix remodelling	2.683
BSK_LPS_MCSF_down	Downregulation of macrophage colony stimulating factor 1 in umbilical vein endothelium and peripheral blood mononuclear cells	Inflammatory cytokine signals	3.048
BSK_SAg_IL8_down	Downregulation of chemokine ligand 8 in umbilical vein endothelium and peripheral blood mononuclear cells	Inflammatory chemokine signals	3.153
BSK_SAg_Proliferation_down	Downregulation of proliferation in umbilical vein endothelium and peripheral blood mononuclear cells	Cell growth regulation	3.434

[1] Additional assay information downloadable at https://www3.epa.gov/research/COMPTOX/toxcast_assay.html

Reprod Toxicol. Author manuscript; available in PMC 2019 August 23.

Table 4.

Comparison of Intermediate Tier Functional and Selected ToxCast HTS Assay Findings

Compound/ Descriptor		Rat Aortic Explant	Rat Whole Embryo	Zebrafish Embryo	Bioseek ToxCast HTS Assay Subset	Tanguay ZF ToxCast HTS Assay Subset	NHEERL ZF 144hpf_ TERATOSCORE_up
Assay Contribution to Embryonic Vascular Disruption MoA		3-D ex vivo primary culture, microvessel outgrowth (reflective of angiogenesis)	Intact organism, embryonic and vascular development (including placental)	Intact organism, embryonic and vascular development (chorion-on)	Human primary cell co-cultures, includes molecular regulators endpoints for vasculogenesis and angiogenesis	High throughput intact zebrafish developmental assay (dechorionated)	Medium throughput intact zebrafish developmental assay (chorion-on)
5HPP-33	**Response Potency (μM)**	1.28	21.2	3.41	Minimum AC50 = 2.90 25th Percentile = 10.87 Median AC50 = 15.2	Active in two assay endpoints. AC50 = 26.2 (Increased mortality), 27.1 (Activity score)	4.44
	Outcome Summary	Disorganized/ degenerate microvessel outgrowth	Embryo lethality	Embryo lethality	Broad activity, anti-proliferative to endothelial cells, cell-cell signaling effects	Embryo lethality, decreased activity	Embryo lethality
TNP-470	**Response Potency (μM)**	0.018	0.038	0.032	Minimum AC50 = 0.001 25th Percentile = 0.45 Median AC50 = 6.2	Minimum AC50 = 0.003 25% Percentile = 0.009 Median AC50 = 0.026	Not active
	Outcome Summary	Stunted microvessel outgrowth, otherwise normal morphology	Dysmorphogenesis, primarily caudal extension defects and abnormal somite patterning	Dysmorphogenesis, primarily caudal extension defects and abnormal somite patterning	Anti-proliferative to endothelial cells, T cells and fibroblasts. Anti-inflammatory, immunomodulatory, and tissue remodeling activity.	Dysmorphogenesis: Caudal fin, axial, pericardial edema, yolk sac defects, eye and jaw defects	Not active